Supporting Information for:

Polymers from sugars and isothiocyanates: ring-opening copolymerization of a D-xylose anhydrosugar oxetane

Ella F. Clark,[a,c] Gabriele Kociok−Köhn,[b] Matthew G. Davidson[a,c] and Antoine Buchard*[a,c]

[a]Department of Chemistry, University of Bath, Claverton Down, Bath, BA2 7AY, UK.

[b]Materials and Chemical Characterisation Facility (MC^2), University of Bath, Claverton Down, Bath, BA2 7AY, UK

[c]University of Bath Institute for Sustainability, Claverton Down, Bath, BA2 7AY, UK.

Email: a.buchard@bath.ac.uk

Contents

1 Materials and Methods

All manipulations were performed under an atmosphere of argon using standard Schlenk techniques unless otherwise stated. (R,R)-1,2-Cyclohexanediamino-N,N'bis(3,5-di-tert-butylsalicyilidene)chromium(III) (**CrSalen**) was purchased from Sigma Aldrich and used without further purification. Bis(triphenylphosphine)iminium chloride (PPNCl) was singly recrystallized from anhydrous acetonitrile prior to use. Anhydrous toluene, σ−dichlorobenzene, acetonitrile, DCM and THF were purchased from Sigma Aldrich. All isothiocyanates were purchased from Fischer Scientific and used without further purification. All other reagents were purchased from either Sigma Aldrich, Alfa Aesar or Acros Organics and used without further purification. All solvents used were anhydrous unless otherwise stated. **D-Ox** was synthesised in three steps from D-xylose according to previous reports.[1, 2] **AlTris**, **FeTris** and **AlPorph** were synthesised according to literature procedures.[3-5]

^{1}H, ^{13}C{^{1}H} and ^{19}F NMR spectra were recorded on a Bruker 400 or 500 MHz instrument and referenced to residual solvent peaks. Coupling constants are given in Hertz. Polymer conversions were determined by ^{1}H NMR spectroscopy by relative integration between monomer and polymer signals.

Mass spectrometry measurements were recorded with a microToF electrospray time of flight (ESI-ToF) mass spectrometer (Bruker Daltonik) in acetonitrile.

THF Size-exclusion chromatography (SEC) was carried out using a THF eluent and processed using multi analysis software. Polymer samples were dissolved at a concentration of 1 mg mL^{-1} in THF and analysed on an Agilent 1260 Infinity series instrument at 1 mL min^{-1} at 35 °C using two PLgel 5 µm MIXED−D 300 × 7.5 mm columns in series. Samples were detected with a differential refractive index (RI) detector. Number-average molar mass ($M_{n,SEC}$), and dispersities, ($Đ_M$ (M_w/M_n)) were calculated against a polystyrene calibration (11 polystyrene standards of narrow molar mass, ranging from M_w 615 - 568000 Da). Data was plotted using Origin 2023.

$CHCl_3$ Size-exclusion chromatography (SEC) was carried out using a $CHCl_3$ eluent and processed using multi analysis software. Polymer samples were dissolved at a concentration of 1 mg mL^{-1} in $CHCl_3$ and analysed on an Agilent 1260 Infinity series instrument at 1 mL min^{-1} at 35 °C using two PLgel 5 µm MIXED-C 300 × 7.5 mm columns in series. Samples were detected with a differential refractive index (RI) detector. Number-average molar mass ($M_{n,SEC}$), and dispersities, ($Đ_M$ (M_w/M_n)) were calculated against a polystyrene calibration (10 polystyrene standards of narrow molar mass, ranging from M_w 855 - 364000 Da). Data was plotted using Origin 2023.

Differential scanning calorimetry (DSC) was carried out using a MicroSC multicell calorimeter from Setaram. The measurement cell and the reference cell were both a 1 mL Hastelloy C cell; a mass of 3-6 mg of polymeric material was loaded into the measurement cell with the reference cell empty. The experiment was performed under nitrogen gas and the sample heated and cooled at a rate of 20 K min^{-1}. A second heating and cooling cycle was carried out immediately following completion of the first. Glass transition temperatures (T_gs) are reported from the second heating cycle unless otherwise stated. The Calisto program was employed to collect and process the data. Data was plotted using Origin 2023.

Thermogravimetric analysis (TGA) was conducted on a Setsys Evolution TGA 16/18 from Setaram. The sample was loaded into a 170 µL alumina crucible and the analytical chamber purged with argon (200 mL min^{-1}) for 40 min prior to starting the analysis. The sample was then heated under an argon flow (20 mL min^{-1}) from 30 to 600 °C at a rate of 2 ˚C min^{-1}. The mass spectrometer was an Omnistar GSD 320 by Pfeiffer Vacuum, equipped with a quadrupole mass analyser and a SEM detector. The Calisto program was employed to collect and process the data. Data was plotted using Origin 2023.

Matrix-assisted laser desorption ionization-time of flight (MALDI-ToF) mass spectrometry was conducted using a Bruker Autoflex speed MALDI Mass Spectrometer equipped with a 2 kHz Smartbeam-II laser. 4.0 mg of DCTB was dissolved in 0.1 mL THF to prepare the matrix solution. 5 mg of poly(**D-Ox**-*alt*-**ITC1**) was dissolved in 1.0 mL of THF to prepare the polymer. The solutions were mixed in a matrix/polymer ratio of 1/1 respectively. 1 µL of the sample mixture were spotted on a 384 well ground steel MALDI target plate and left to dry before being inserted into the MALDI instrument. Once loaded, positive ion MALDI spectra were obtained in linear mode. Laser intensity was varied. The data was analysed using the Flex Analysis software, version 3.4 (build 76). The molar mass distributions were obtained through analysis of the data in the Polytools software package 1.31.

LC-MS analysis was performed using an Agilent QTOF 6545 with Jetstream ESI spray source coupled to an Agilent 1260 Infinity II Quat pump HPLC with 1260 autosampler, variable wavelength detector (VWD) and column oven compartment. The MS was operated in positive mode with the drying gas, the gas temperature and the nebulizer gas at 12 L min^{-1}, 250°C and 45 psi (3.10 bar) respectively. The sheath gas flow and temperature were set to 12 L min^{-1} and 350°C, respectively. The MS was calibrated using reference calibrant from the independent ESI reference sprayer. The VCap, Skimmer and Fragmentor was set to 3500, 45 and 125 respectively.

FT-IR analysis was done using a PerkinElmer Inc. Spectrum 100 FT-IR Spectrometer. Universal ATR enabling wavelengths from 650-4000 cm^{-1} (15 µm to 2.5 µm).

In-situ IR analysis was done using a ReactIR 702L system from Mettler Toledo; measurements were recorded using a DiComp (Diamond) IR probe and TE MCT detector over a sampling range of 3000-650 cm^{-1}. The iC IR 7.1 Office software was employed to collect and process the data.

Raman analysis was done using a Tornado Spectral Systems HyperFlux PRO Plus 785; measurements were recorded using a 1/2" Process BallProbe with sapphire lens and 785nm laser, max power 495mW over a sampling range of 200-3300cm^{-1}. The SpectralSoft™ software was employed to collect and process the data.

Single-Crystal X-ray Diffraction (XRD) analysis was carried out at 150(2) K on a Rigaku SuperNova, EosS2 single crystal diffractometer using monochromated CuKα radiation (λ = 1.5418 Å). Unit cell determination, data collection and data reduction were performed using the CrysAlisPro software. The structure was solved with SHELXT and refined by a full-matrix least-squares procedure based on F^2 (SHELXL-2018/3)[6]. All non-hydrogen atoms were refined anisotropically. Hydrogen atoms were placed onto calculated positions and refined using a riding model.

Photoreactors: All batch photoreactions were conducted in commercially−available EvoluChemPhotoRedOx Box reactors purchased from HepatoChem Inc.(100 Cummings Center, Suite 451C, Beverly, MA 01915 USA). The light source employed in this work was a 365DX LED (λ = 365 nm; 25 mW/cm2), purchased from HepatoChem Inc.

2 General Procedures

2.1 General procedure 3,5-bis(trifluoromethyl)phenyl isothiocyanate (ITC1)/D-Ox ROCOP

Under an argon atmosphere, **AlTris** (40 µL, 0.125 mol L^{-1} solution in anhydrous THF, 5 x 10^{-3} mmol, 1.00 equiv.), PPNCl (20 µL, 0.25 mol L^{-1} solution in anhydrous DCM, 5 x 10^{-3} mmol, 1.00 equiv.) and 3,5-Bis(trifluoromethyl)phenyl isothiocyanate (271 mg, 1 mmol, 200.00 equiv.) were added to a 1.52 mol L^{-1} toluene solution of **D-Ox** (172 mg, 1 mmol, 200.00 equiv.). The vial was sealed and heated to 80 °C with stirring. After 48 hours the vial was cooled, and the polymerisation was quenched by exposing the reaction to air. The resultant product was dissolved in $CHCl_3$ (2 mL) before precipitation of the product with cold methanol. The suspension was then centrifuged (3000 rpm, 5 minutes), the polymer was collected and dried *in vacuo* at 40 °C to yield the poly(**D-Ox**-*alt*-**ITC1**) (79 % yield, 0.3515 g).

2.2 General procedure for synthesis of C1

Under an argon atmosphere, **AlPorph** (240 µL, 0.125 mol L^{-1} solution in anhydrous THF, 3 x 10^{-2} mmol, 1.00 equiv.), PPNCl (120 µL, 0.25 mol L^{-1} solution in anhydrous DCM, 3 x 10^{-2} mmol, 1.00 equiv.) and 3,5-Bis(trifluoromethyl)phenyl isothiocyanate (813 mg, 1 mmol, 100.00 equiv.) were added to a 1.52 mol L^{-1} *σ*–dichlorobenzene solution of **D-Ox** (516 mg, 1 mmol, 100.00 equiv.). The vial was sealed and heated to 120 °C with stirring. After 48 hours the vial was cooled, and the polymerisation was quenched with $CHCl_3$ (5 mL) and any oligomeric species were precipitated from cold hexane. The supernatant was left to slowly evaporate, and the crystals were collected and dried *in vacuo* at 40 °C to yield **C1**, (8 % yield, 0.1063 g).

2.3 Degradation of poly(D-Ox-*alt*-ITC1)

Poly(**D-Ox**-*alt*-**ITC1**) (50 mg) was added to a 1 mol L^{-1} solution of either $HCl_{(aq)}$ or $NaOH_{(aq)}$ in THF (2.5 mL) and stirred at 50 °C for 5 hours, with samples (0.4 mL) taken every hour. All crude samples were dried and then subjected to ^1H NMR spectroscopy and SEC analysis.

2.4 Degradation of poly(D-Ox-*alt*-ITC1) under UV light.

Poly(**D-Ox**-*alt*-**ITC1**) (50 mg) was dissolved in THF (2.5 mL) and stirred at room temperature under UV light (λ = 365 nm), with samples (0.4 mL) taken at predetermined intervals. All crude samples were dried and then subjected to ^1H NMR spectroscopy and SEC analysis.

2.5 General procedure for alcohol initiated ITC1/D-Ox ROCOP

Under an argon atmosphere, **AlTris** (80 µL, 0.125 mol L^{-1} solution in anhydrous THF, 1 x 10^{-2} mmol, 2.00 equiv.), DBU (20 µL, 0.5 mol L^{-1} solution in anhydrous DCM, 1 x 10^{-2} mmol, 2.00 equiv.), 1,4-butanediol (50 µL, 1 mol L^{-1} solution in anhydrous MeCN, 5 x 10^{-3} mmol, 1.00 equiv.), and 3,5-bis(trifluoromethyl)phenyl isothiocyanate (271 mg, 1 mmol, 200.00 equiv.) were added to a 1.52 mol L^{-1} toluene solution of **D-Ox** (172 mg, 1 mmol, 200.00 equiv.). The vial was sealed and heated to 80 °C with stirring. After 24 hours the vial was cooled, and the polymerisation was quenched by exposing the reaction to air. The resultant product was dissolved in $CHCl_3$ (2 mL) before precipitation of the

product with cold methanol. The suspension was then centrifuged (3000 rpm, 5 minutes), the polymer was collected and dried *in vacuo* at 40 °C to yield the poly(**D-Ox**-*alt*-**ITC1**).

2.6 General Procedure for poly(LLA-*b*-(D-Ox-*alt*-ITC1)-*b*-LLA)

Under an argon atmosphere, **AlTris** (320 µL, 0.125 mol L^{-1} solution in anhydrous THF, 4 x 10^{-2} mmol, 2.00 equiv.), DBU (80 µL, 0.5 mol L^{-1} solution in anhydrous DCM, 4 x 10^{-2} mmol, 2.00 equiv.), 1,4-butanediol (200 µL, 1 mol L^{-1} solution in anhydrous MeCN, 2 x 10^{-2} mmol, 1.00 equiv.), and 3,5-bis(trifluoromethyl)phenyl isothiocyanate (271 mg, 1 mmol, 200.00 equiv.) were added to a 1.52 mol L^{-1} toluene solution of **D-Ox** (172 mg, 1 mmol, 200.00 equiv.). The vessel was sealed and stirred at 80 °C. After 18 hours a sample was taken and L-lactide (576 mg, 4 mmol, 800.00 equiv.) was added under a flow of argon. The vessel was resealed and stirred for 24 hours after which, the polymerisation was quenched with $CHCl_3$ (2 mL). The product was precipitated from cold methanol, centrifuged (3000 rpm, 5 minutes), collected and dried *in vacuo* at 40 °C to yield poly(LLA-*b*-(**D-Ox**-*alt*-**ITC1**)-*b*-LLA).

2.6 General procedure for metal coordination

Poly(**D-Ox**-*alt*-**ITC1**) (50 mg) was added to of a 1 mol L^{-1} solution of the metal precursor in water. The suspension was stirred at 80 °C for 24 hours. The solution was then diluted to 5.5 x 10^{-3} mol L^{-1} of the metal complex and centrifuged (3000 rpm, 5 minutes). This was repeated three times, with stirring to form a suspension between each centrifugation. The product was finally collected and dried *in vacuo* at 50 °C to yield polymer−M.

3 Catalyst Screening

3.1 Table of catalyst screening data

Table S1. Catalyst Screening

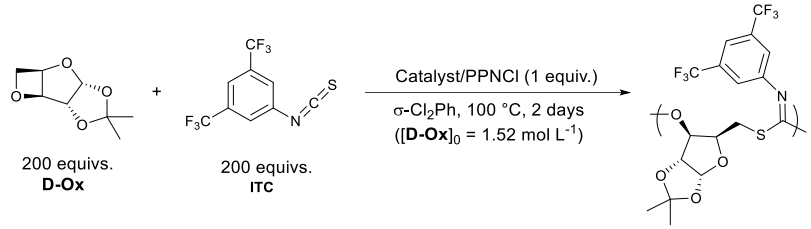

catalyst/initiator systems tested:

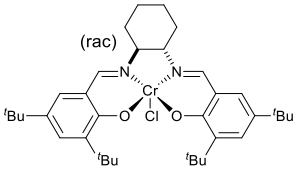

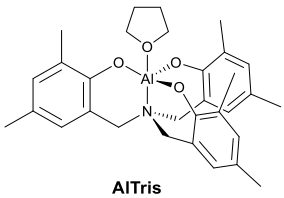

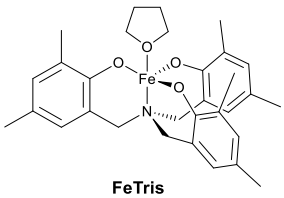

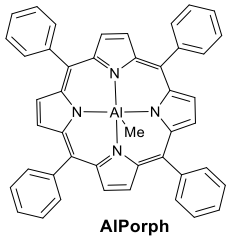

Entry	Cyclic Ether	Catalyst[a]	Time (h)	Conv (%)	Select[c] (%)	$M_{n,theo}$	$M_{n,SEC}$ [d] ($Đ_M$)
1	**D-Ox**	**CrSalen**	48	22	77	19,500	7,000 (1.28)
2	CHO	**CrSalen**	48	>99	>99	73,100	15,000 (1.29)
3	**D-Ox**	**AlTris**	48	>99	63	55,000	21,000 (1.63)
4	CHO	**AlTris**	48	71	>99	52,400	20,000 (1.45)
5	**D-Ox**	**AlTris**	6	84	98	72,700	21,300 (1.63)
6	**D-Ox**	**FeTris**	48	>99	88	78,000	16,100 (1.46)
7	**D-Ox**	**FeTris**	6	85	93	70,000	15,900 (1.62)
8	**D-Ox**	**AlPorph**	48	>99	20	17,800	4,000 (1.10)
9	**D-Ox**	**AlPorph**	6	56	12	6,200	2,000 (1.09)

[a]Reactions carried out at [**D-Ox**]$_0$ = 1.52 mol L^{-1} in σ−dichlorobenzene with a 200:200:1:1 ratio of **D-Ox**:**ITC**:cat:**PPNCl** and **CHO**:**ITC**:cat:**PPNCl** unless otherwise stated. [b]Conversion of **D-Ox** determined by ^{1}H NMR spectroscopy by relative integration of anomeric protons in **D-Ox** ($CDCl_3$, δ = 6.26 ppm (d, *J* = 3.7 Hz)) and poly(**D-Ox**-*alt*-**ITC1**) ($CDCl_3$, δ = 5.81 ppm (m), conversion of CHO determined by ^{1}H NMR spectroscopy by relative integration of protons in CHO ($CDCl_3$, δ = 3.12 ppm (m)) and poly(CHO-*alt*-**ITC1**) ($CDCl_3$, δ = 5.5-5.0 ppm (m)). [d] Percentage of converted **D-Ox** and CHO to poly(**ITC1**-*alt*-**D-Ox**) and poly(**ITC1**-*alt*-CHO) respectively. Calculated by SEC relative to polystyrene standards in THF eluent, $Đ_M = M_w/M_n$.

4 Characterisation of Poly(D-Ox-*alt*-ITC1)

4.1 NMR analysis of poly(D-Ox-*alt*-ITC1)

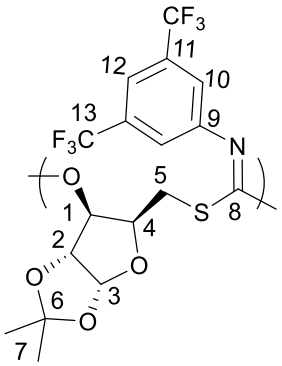

Poly(imidothiocarbonate): white solid; 79 % yield (0.3515 g).

^{1}H NMR (500 MHz, $CDCl_3$) δ (ppm): 7.58 (s, 1H, H−12), 7.21 (m, 2H, H−10), 5.88 (m, 1H, H−3), 5.51 (m, 1H, H−1), 4.71 (m, 9H, H−2), 4.42 (m, 1H, H−4), 3.20−3.00 (m, 2H, H−5), 1.44 (m, 3H, H−7), 1.44 (m, 3H, H−7).

^{13}C{^{1}H} NMR (126 MHz, $CDCl_3$) δ (ppm): 158.0 (C−8), 147.2 (C−9), 132.8 (C−11), 124.2 (C−13), 121.7 (C−10), 118.0 (C−12), 112.6 (C−6), 104.6 (C−3), 82.9 (C−2), 80.6 (C−1), 78.6 (C−4), 28.6 (C−5), 26.5 (C−7), 26.0 (C−7).

FTIR ν_{max} (cm^{-1}): 1632 (C=N), 1379 (C-H_3), 1278 ($C_{aromatic}$-N) 1134 (C-S).

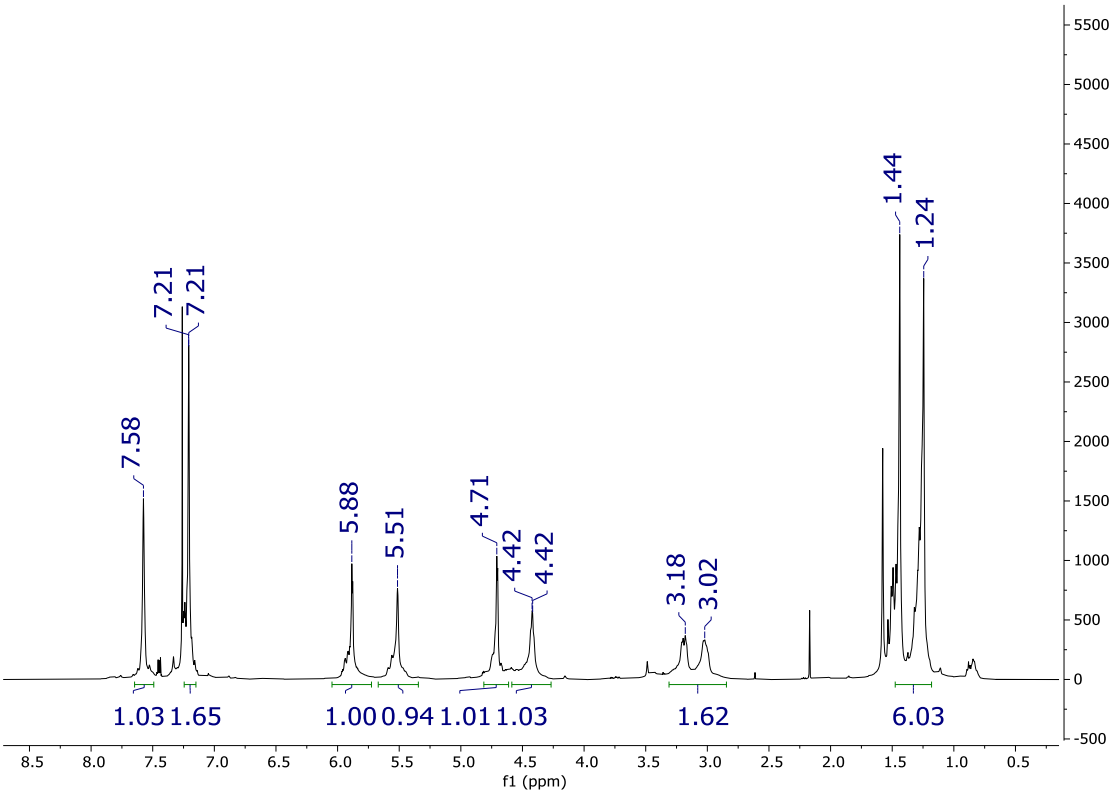

Fig. S1 ^{1}H NMR spectrum ($CDCl_3$) of poly(**D-Ox**-*alt*-**ITC1**) ($CHCl_3$, acetone and water residual signal at 7.26, 2.17 and 1.56 ppm respectively).

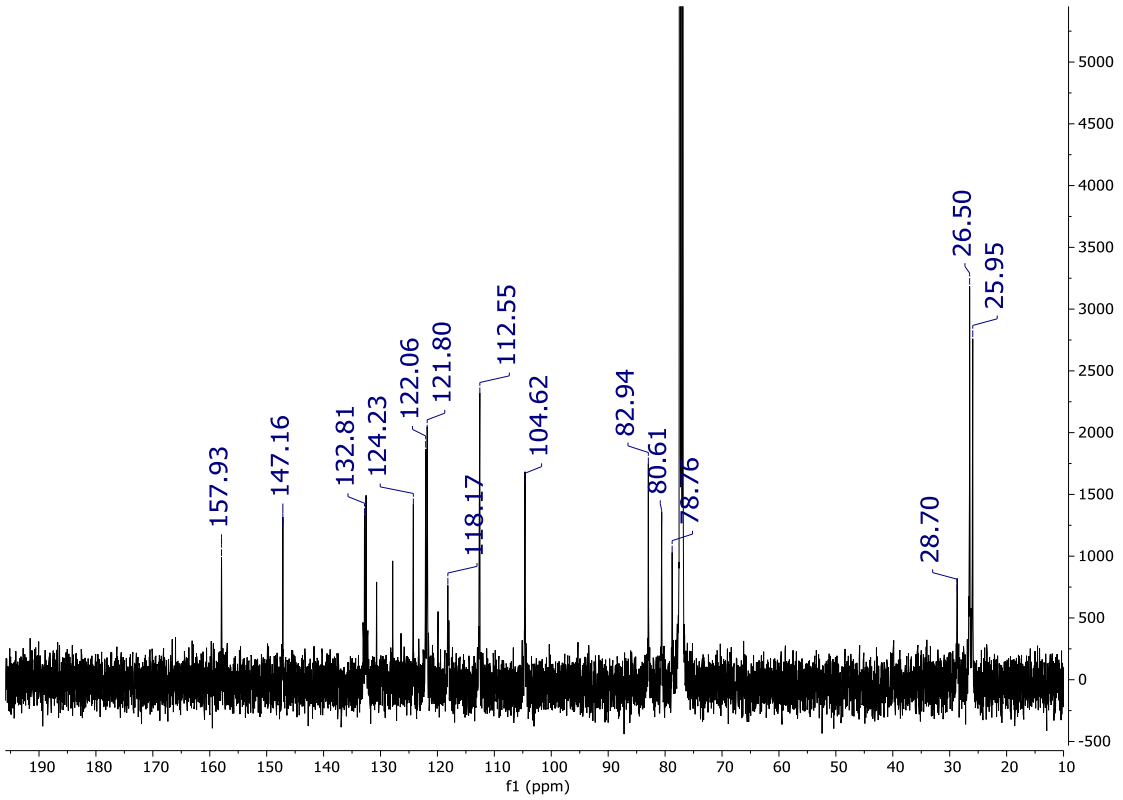

Fig. S2 $^{13}C\{^{1}H\}$ NMR spectrum ($CDCl_3$) of poly(**D-Ox**-*alt*-**ITC1**) (1.2-dichlorobenzene and $CHCl_3$ residual signals at 132.54, 130.69, 127.86 and 77.16 ppm respectively).

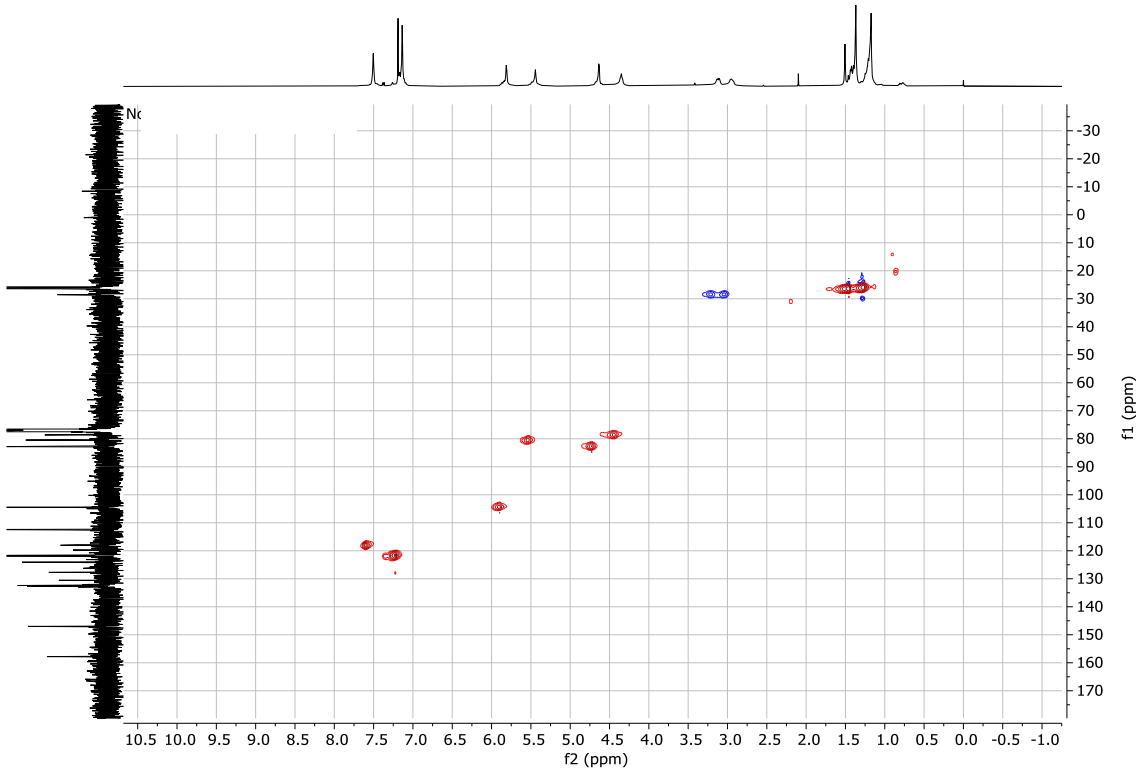

Fig. S3 ^{1}H-$^{13}C\{^{1}H\}$ HSQC NMR spectrum ($CDCl_3$) of poly(**D-Ox**-*alt*-**ITC1**).

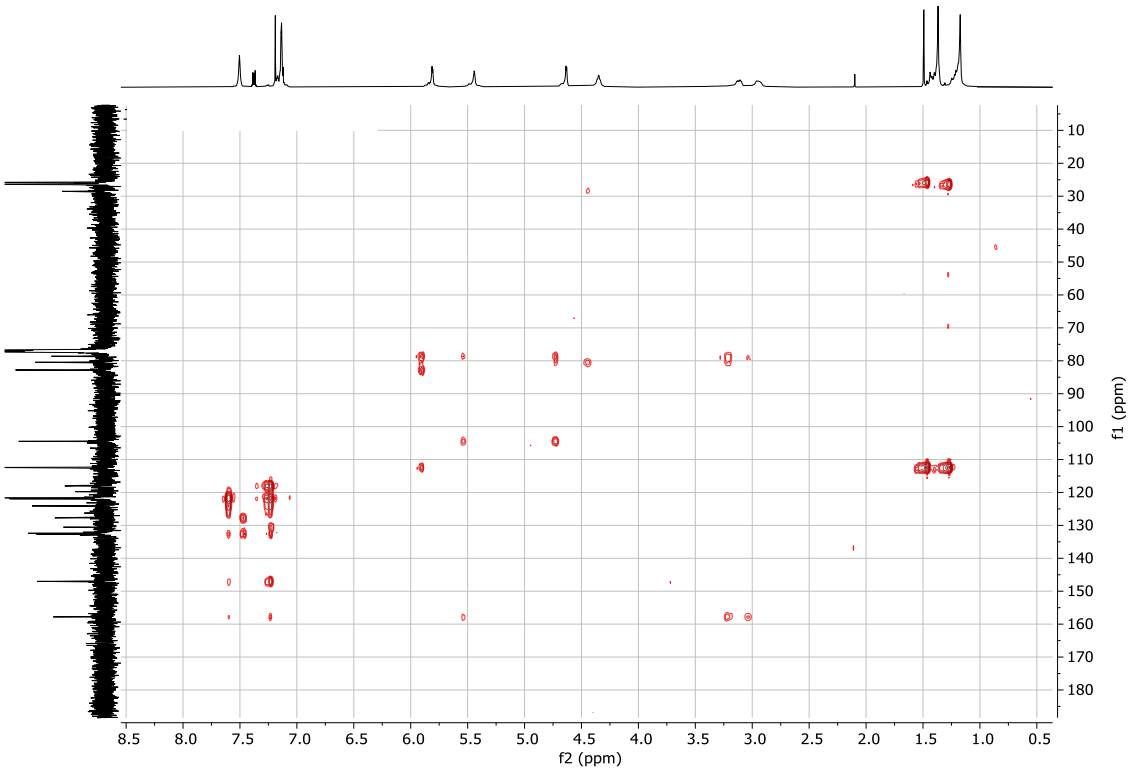

Fig. S4 ^{1}H-^{13}C{^{1}H} HMBC NMR spectrum ($CDCl_3$) of poly(**D-Ox**-*alt*-**ITC1**).

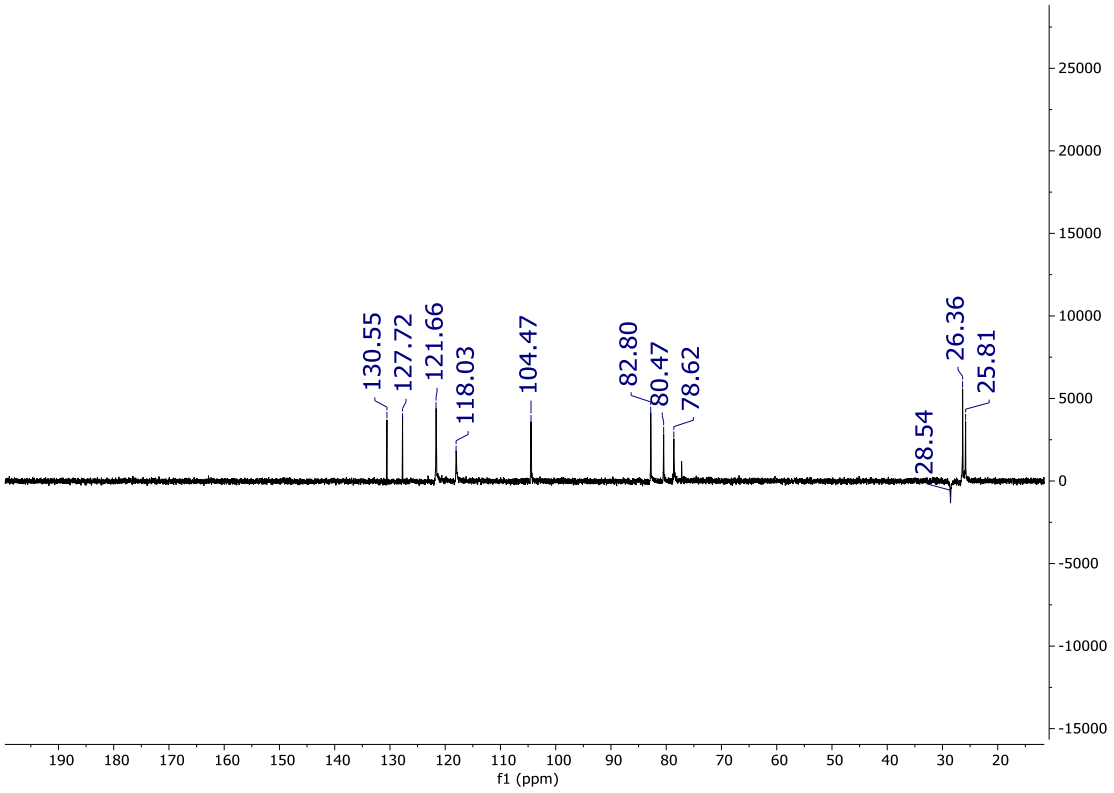

Fig. S5 ^{13}C{^{1}H} DEPT 135 NMR spectrum ($CDCl_3$) of poly(**D-Ox**-*alt*-**ITC1**).

4.2 FTIR analysis of poly(D-Ox-*alt*-ITC1)

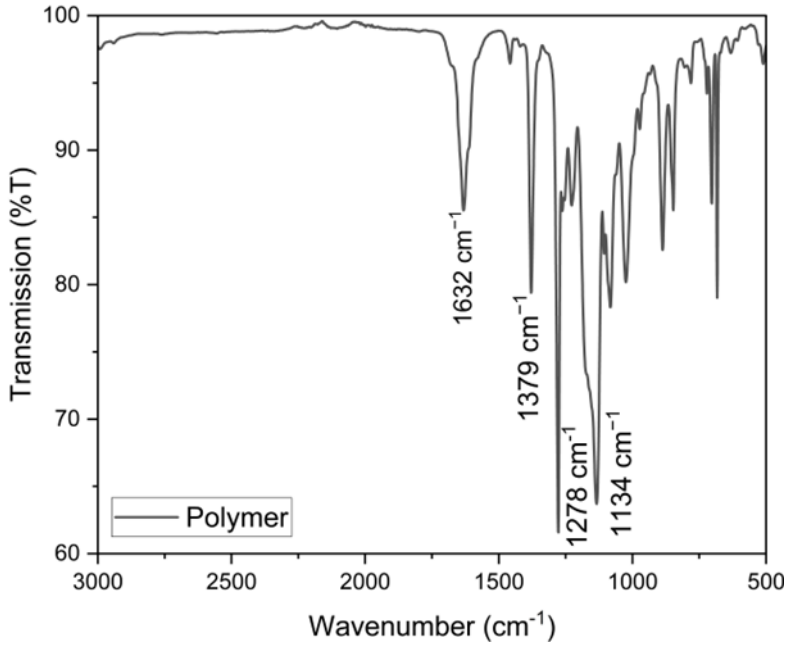

Fig. S6 FTIR spectrum of poly(**D-Ox**-*alt*-**ITC1**).

4.3 Size-exclusion chromatography analysis of poly(D-Ox-*alt*-ITC1)

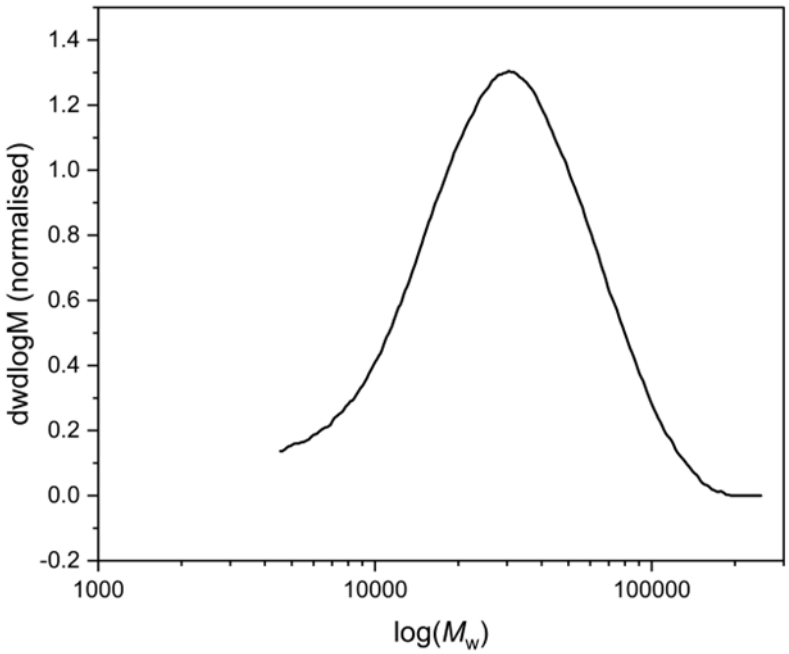

Fig. S7 SEC trace for the ROCOP of **D-Ox** and **ITC1** by **AlTris** (*DP* ~50, $M_{n,SEC}$= 22,000 g mol^{-1}, $Đ_M$ = 1.63).

4.4 Thermal analysis of poly(D-Ox-*alt*-ITC1)

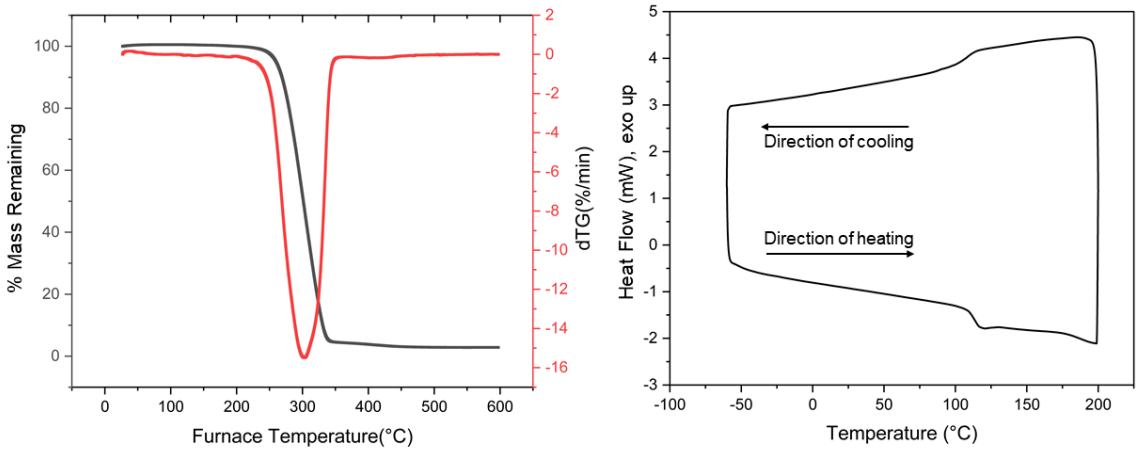

Fig. S8 (left) TGA (black = % mass loss, red = derivative of % mass loss) and (right) DSC (second cooling and second heating cycles) of poly(**D-Ox**-*alt*-**ITC1**) $M_{n,SEC}$ = 18,700 g mol^{-1}, $Đ_M$ =1.37; T_g = 114 °C; $T_{d,5\%}$ = 260 °C; with 3% char remaining at 600 °C, measured under argon atmosphere.

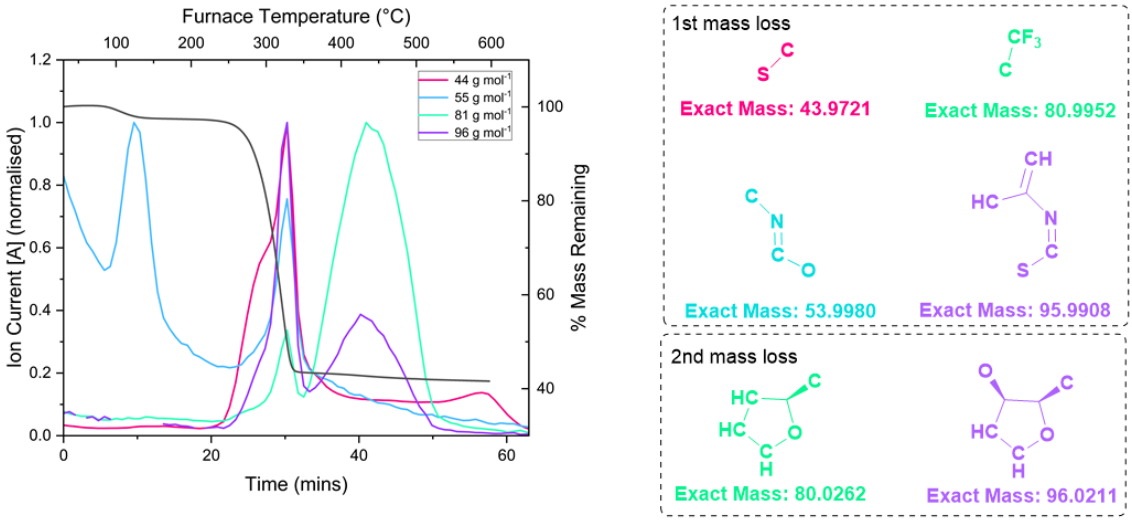

Fig. S9(left) TGA (black = % mass loss, pink, blue, green, and purple are the ion current at 44, 55, 81 and 96 g mol^{-1} respectively) of poly(**D-Ox**-*alt*-**ITC1**) and (right) suggested decomposition structures.

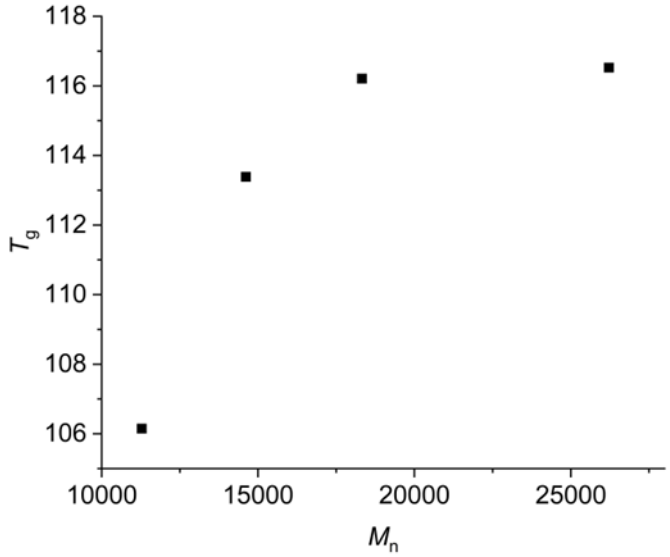

Fig. S10 Plot of molar mass *vs* T_g obtained from the second heating cycle in the DSC thermogram for samples of poly(**D-Ox**-*alt*-**ITC1**).

4.5 MALDI-ToF mass spectrometry of poly(D-Ox-*alt*-ITC1)

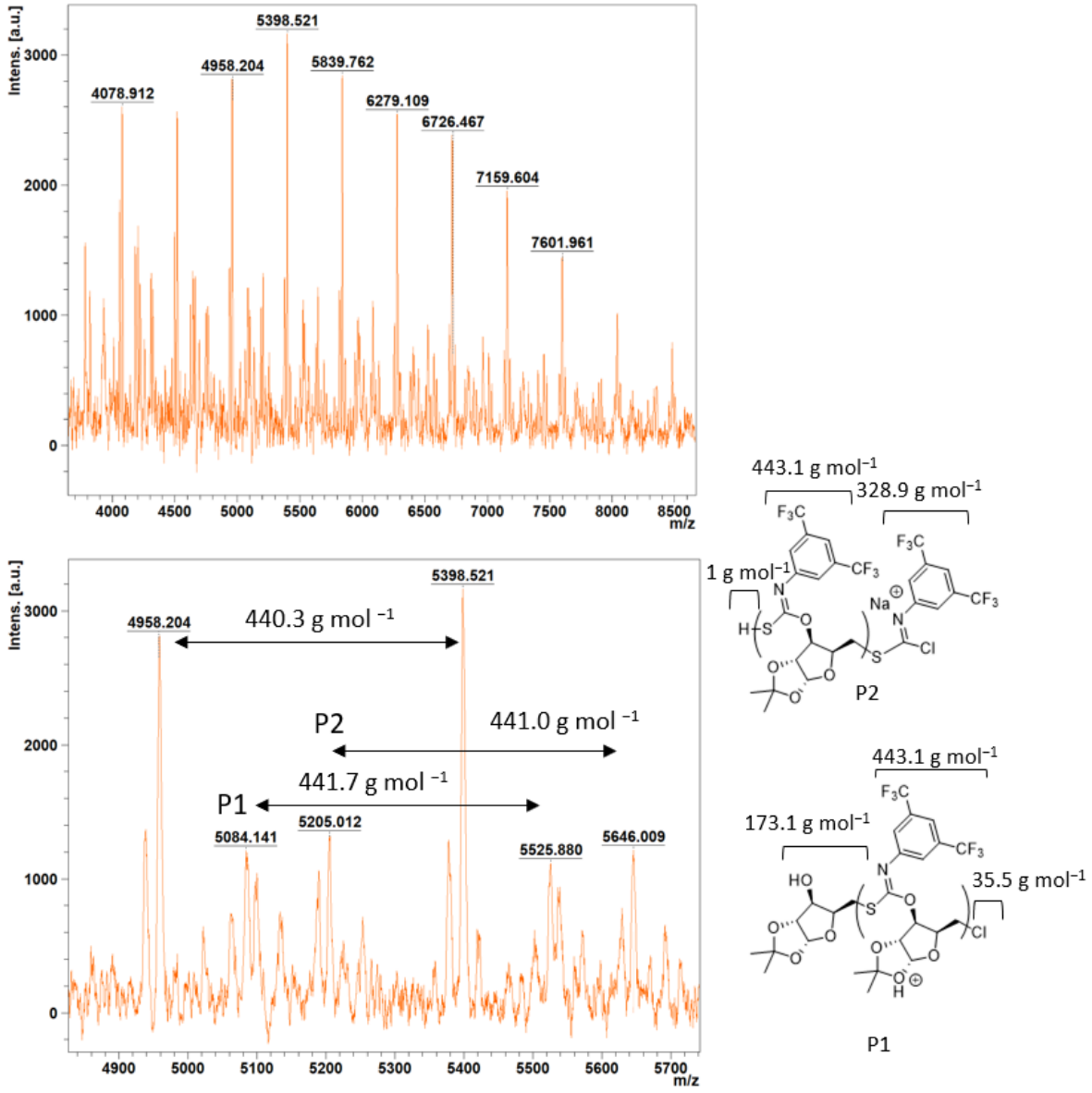

Fig S11 MALDI−ToF mass spectrum of poly(**D-Ox**-*alt*-**ITC1**).

4.6 Conversion of D-Ox *vs* $M_{n,SEC}$ plot

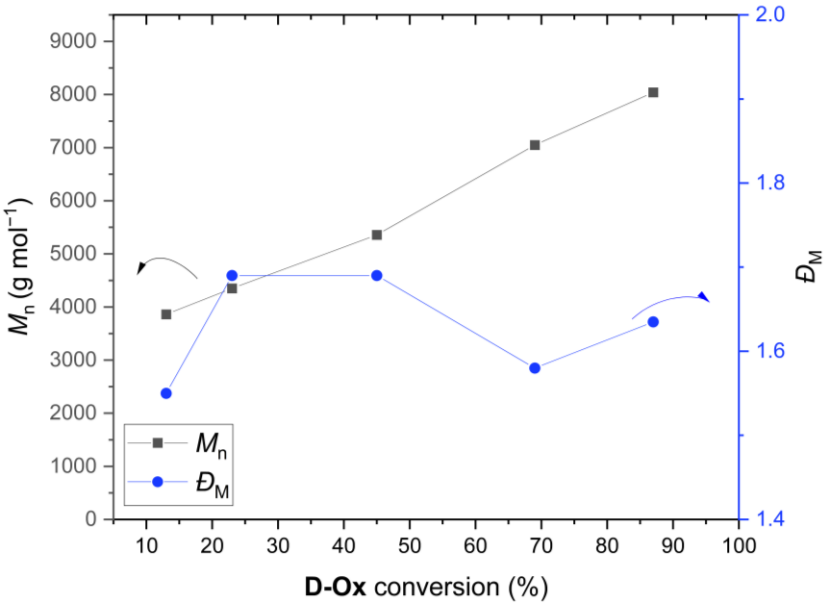

Fig. S12 Conversion of **D-Ox** *vs* $M_{n,SEC}$ (black) and $Đ_M$ (red). Reaction performed in toluene at 80 °C with at [**D-Ox**]$_0$:[**ITC**]$_0$:[**CrSalen**]$_0$:[PPNCl]$_0$ loadings of 200:200:1:1. [**D-Ox**]$_0$ = 1.52 mol L^{-1}.

4.7 DOSY NMR analysis of the crude polymerisation of D-Ox and ITC1

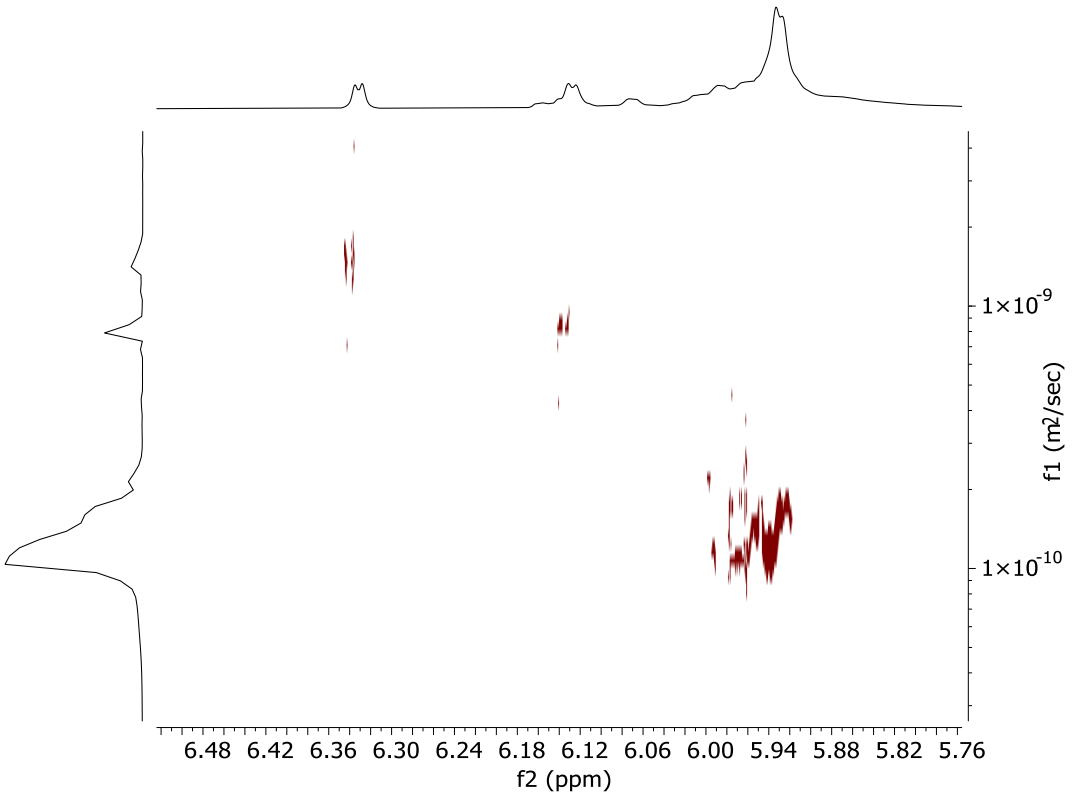

Fig. S13 ^{1}H DOSY NMR spectrum ($CDCl_3$) of crude sample of the polymerisation of **D-Ox** (6.33 ppm, 1.41 x 10^{-9} m^2 s^{-1})and **ITC1** to form poly(**D-Ox**-*alt*-**ITC1**) (5.95 ppm, 1.21 x 10^{-10} m^2 s^{-1}) and **C1** (6.13 ppm, 8.01 x 10^{-10} m^2 s^{-1}), catalysed by **CrSalen**. Zoomed into the anomeric region.

4.7 ROCOP living character

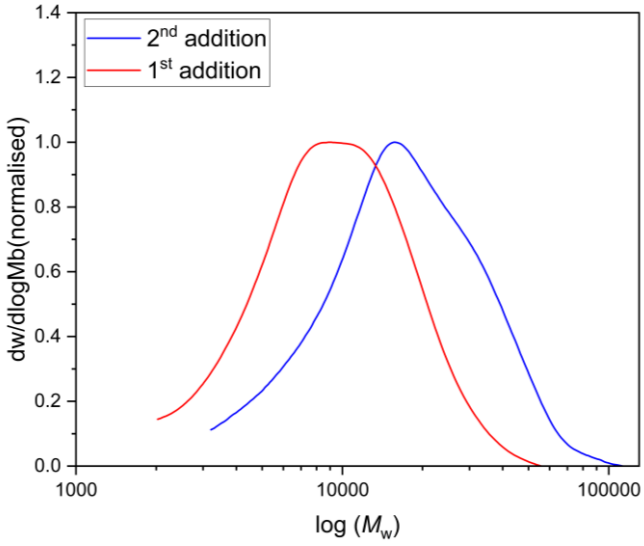

Fig. S14 SEC traces (THF eluent) from the sequence addition polymerisation of **D-Ox** and **ITC1.** $M_{n,SEC}$ before second monomer batch addition = 7,600 g mol^{-1}, $Đ_M$ = 1.47, $M_{n,SEC}$ after second monomer batch addition = 13,300 g mol^{-1}, $Đ_M$ = 1.56.

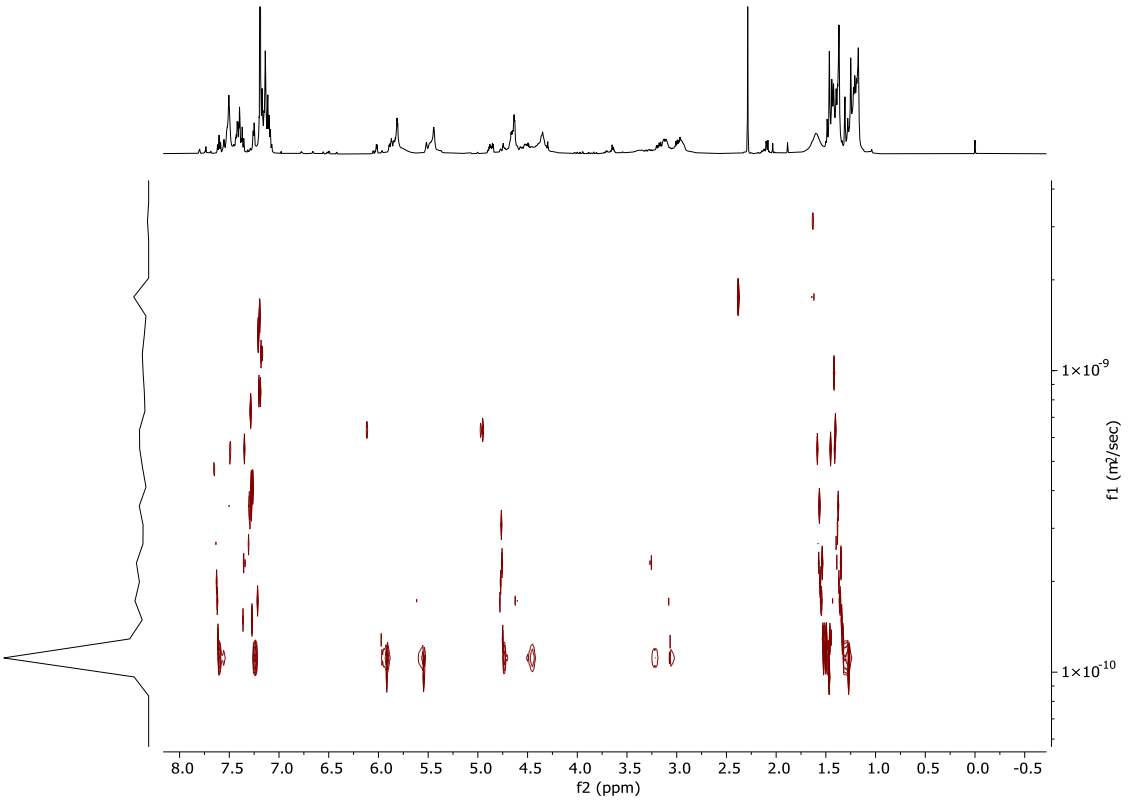

Fig. S15 ^{1}H DOSY NMR spectrum ($CDCl_3$) of crude sample of the sequence addition polymerisation of **D-Ox** and **ITC1** to form poly(**D-Ox**-*alt*-**ITC1**) (1.11 ×10^{-11} m^2 s^{-1}).

5 Characterisation of C1

5.1 NMR analysis of C1

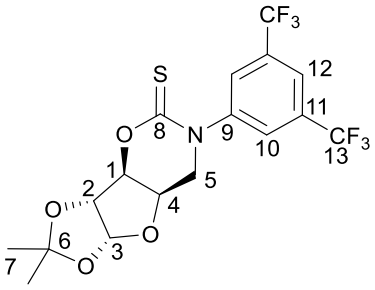

C1: white solid; 8 % yield (0.1063 g).

^{1}H NMR (500 MHz, $CDCl_3$, δ (ppm): 7.87 (s, 1H, H−12), 7.80 (s, 2H, H−10), 6.12 (d, J = 3.25 Hz, 1H, H−1), 4.94 (m, 2H, H−2, H-1), 4.84 (m, 1H, H−4), 4.05 – 3.86 (m, 2H, H−5), 1.56 (s, 3H, H−7), 1.38 (s, 3H, H−7).

^{13}C{^{1}H} NMR (126 MHz, $CDCl_3$, δ (ppm): 185.7 (C−8), 146.5 (C−9), 133.6 (C−11), 133.3 (C−13), 128.3 (C−10), 122.4 (C−12), 113.4 (C−6), 105.5 (C−3), 83.8 (C−2), 82.7 (C−1), 70.6 (C−4), 50.9 (C−5), 26.9 (C−7), 26.4 (C−7).

FTIR ν_{max} (cm^{-1}): 1485 (C=S), 1380 (C-H_3), 1276 ($C_{aromatic}$-N) 1122 (C-N).

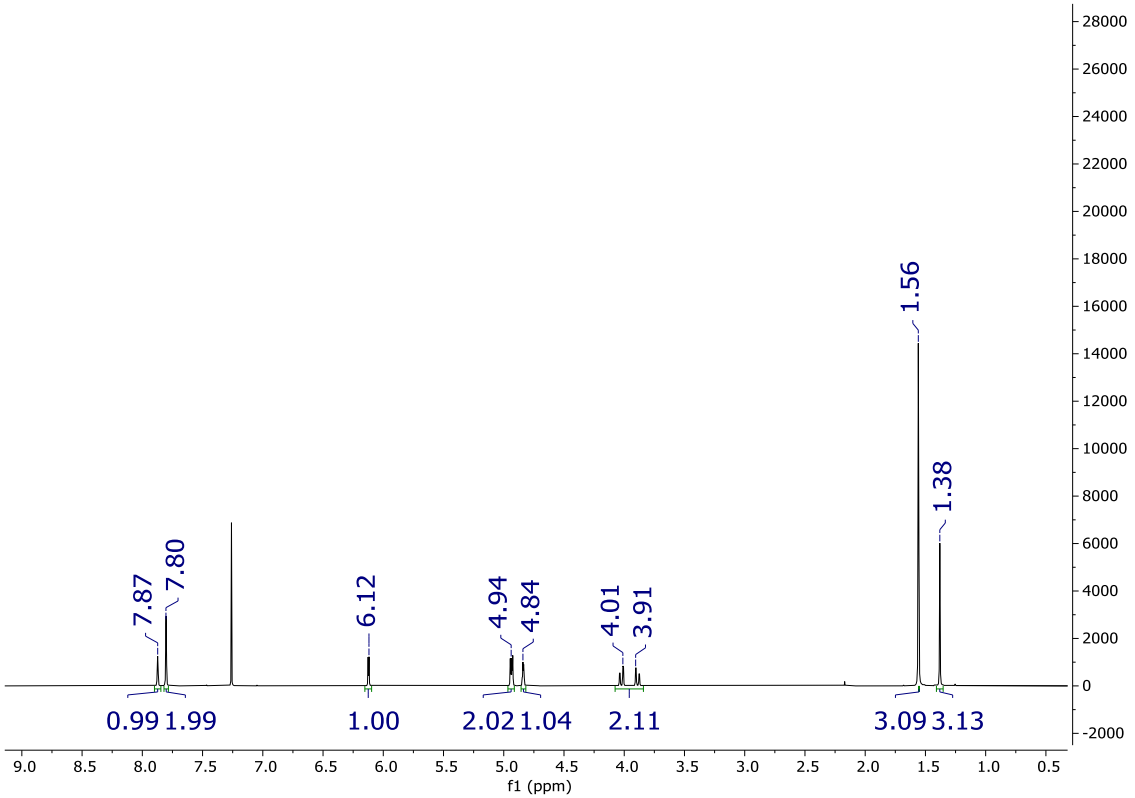

Fig. S16 ^{1}H NMR spectrum ($CDCl_3$) of **C1** ($CHCl_3$ residual signal at 7.26 ppm).

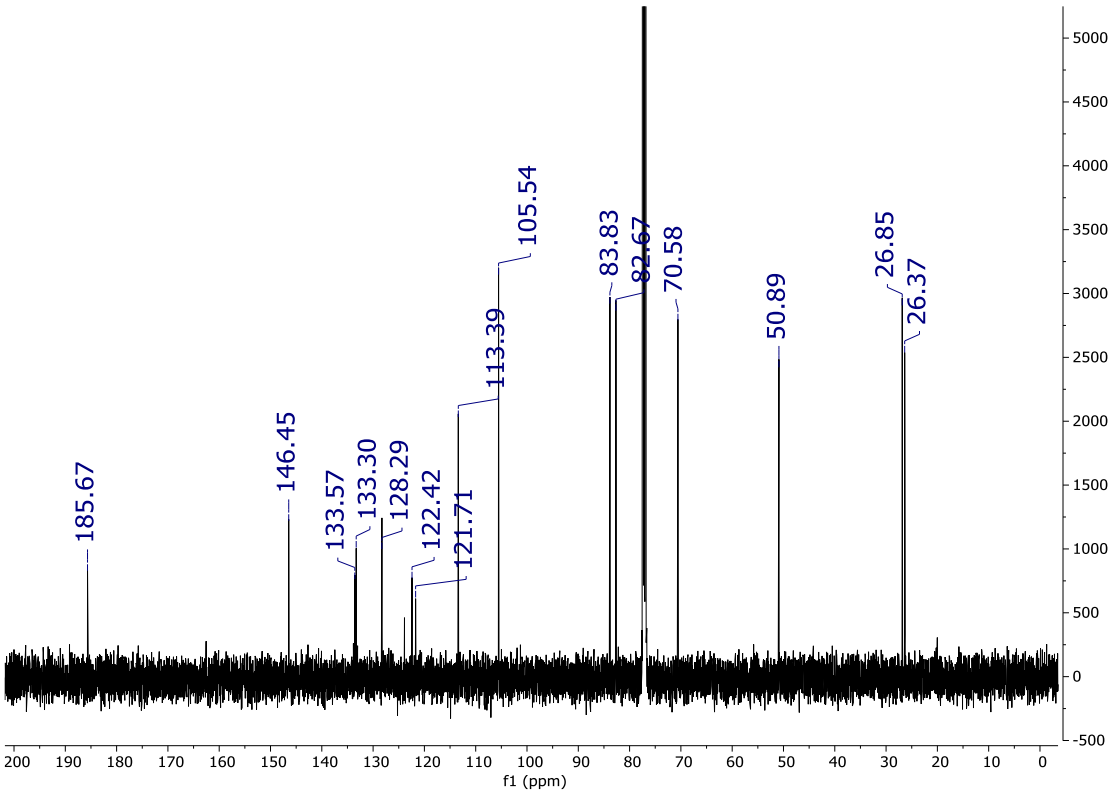

Fig. S17 $^{13}C\{^{1}H\}$ NMR spectrum ($CDCl_3$) of **C1** (σ−dichlorobenzene and $CHCl_3$ residual signal at 132.77.16 and 77.16 ppm respectively).

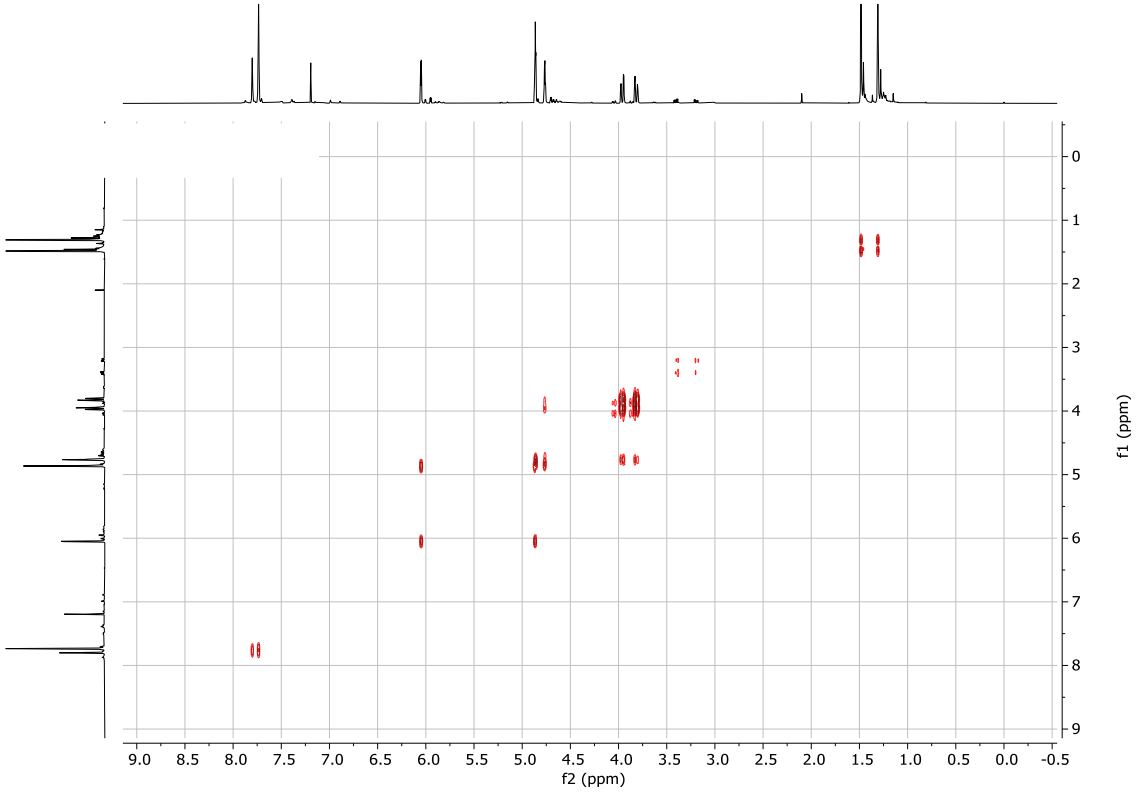

Fig. S18 ^{1}H COSY NMR spectrum ($CDCl_3$) of **C1** ($CHCl_3$ residual signal at 7.26 ppm).

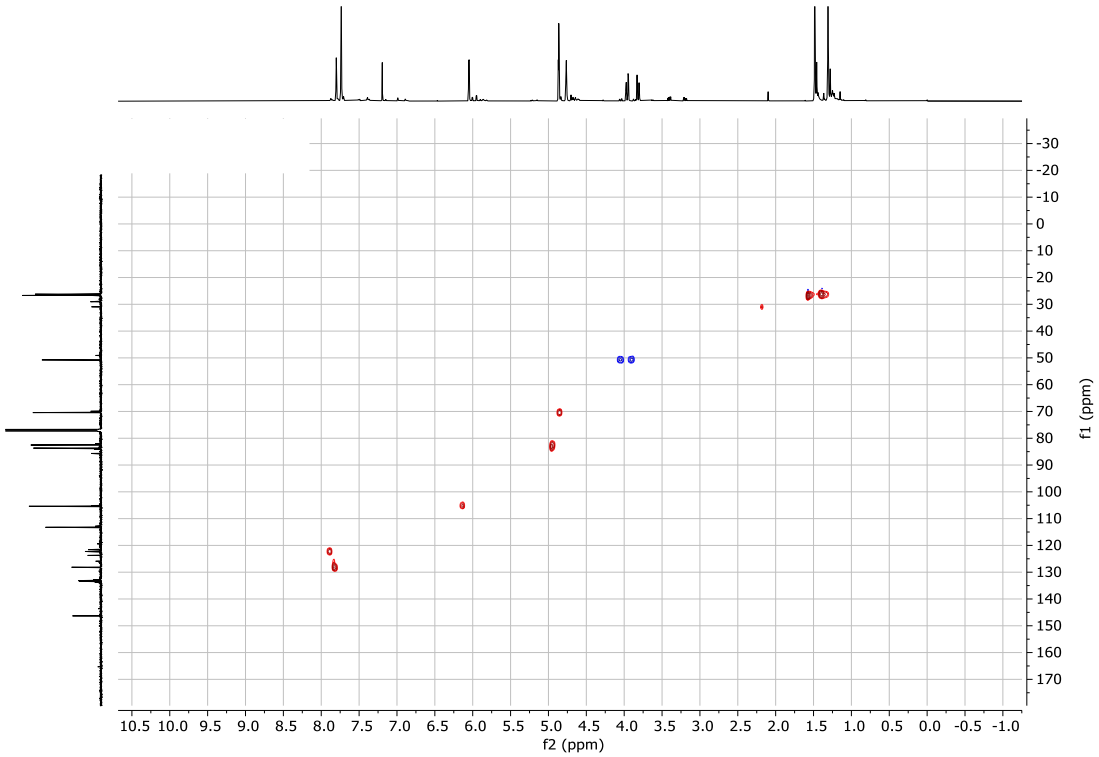

Fig. S19 ^{1}H-^{13}C{^{1}H} HSQC NMR spectrum ($CDCl_3$) of **C1** (residual acetone peak at 2.17).

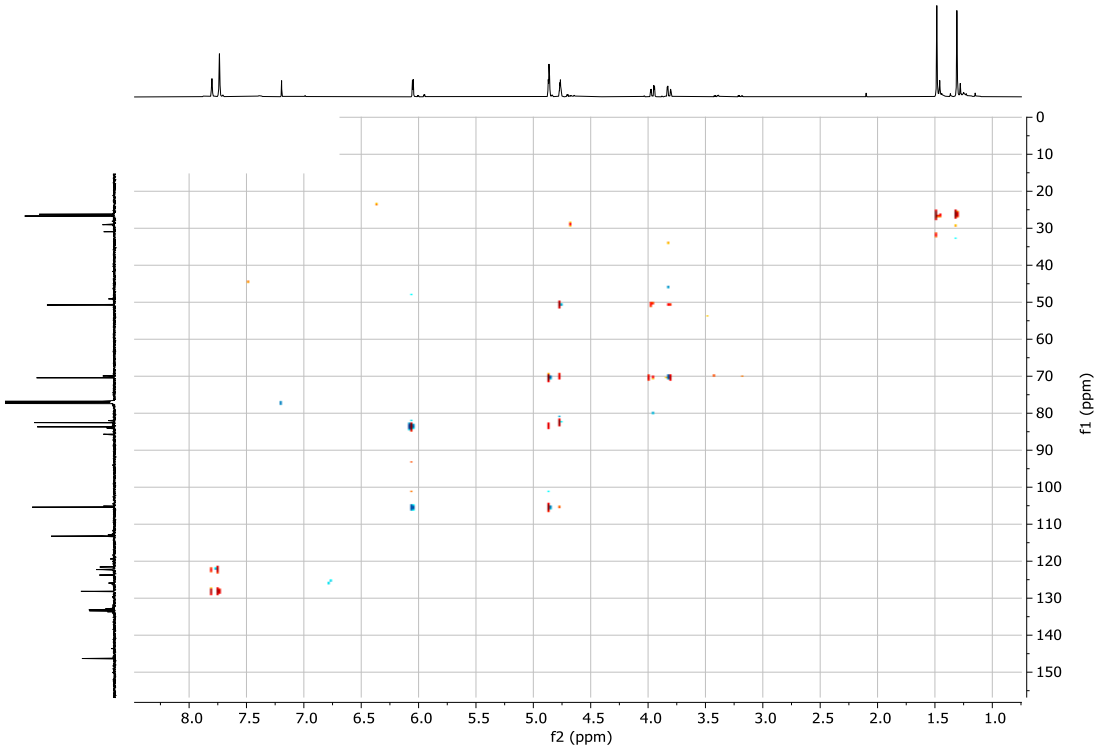

Fig. S20 ^{1}H-^{13}C{^{1}H} HMBC NMR spectrum ($CDCl_3$) of **C1**.

5.2 Crystal structure of C1.

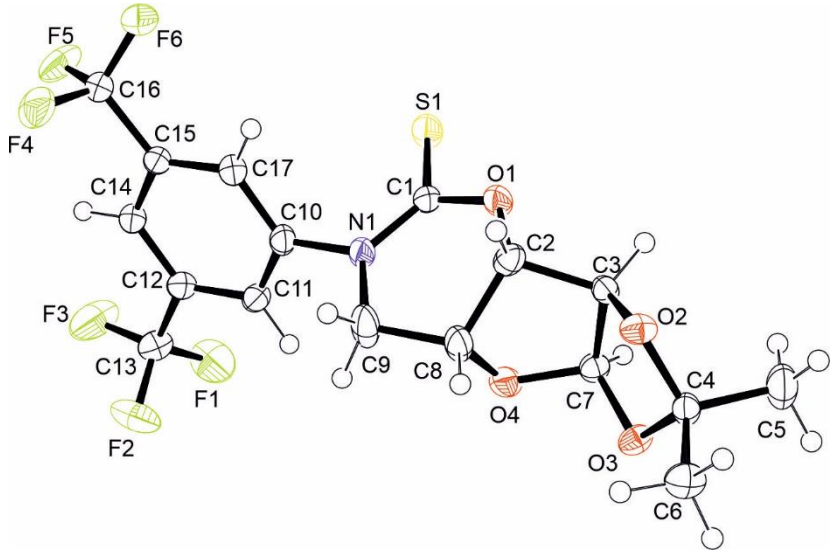

Fig. S21 ORTEP drawing of the crystal structure of **C1** with thermal ellipsoids at the 50% probability level. Selected bond lengths (Å): S(02) – C(19) 1.687, N(14) – C(19) 1.356, O(20) – C(19) 1.324. Selected bong angles (°): C(1)-N(1)-C(10) 119.6(3), C(1)-N(1)-C(9) 124.5(3), C(10)-N(1)-C(9), 115.8(3) O(1)-C(1)-N(1), O(1)-C(1)-S(1) 116.1(2), N(1)-C(1)-S(1) 124.7(2).

Identification code	s22ab2	
Empirical formula	C17 H15 F6 N O4 S	
Formula weight	443.36	
Temperature	150.01(10) K	
Wavelength	1.54184 Å	
Crystal system	Monoclinic	
Space group	$P2_1$	
Unit cell dimensions	a = 5.47055(6) Å	a= 90°.
	b = 23.5365(3) Å	b= 94.2334(10)°.
	c = 14.44919(14) Å	g = 90°.
Volume	1855.37(4) $Å^3$	
Z	4	
Density (calculated)	1.587 Mg/m^3	
Absorption coefficient	2.347 mm^{-1}	
F(000)	904	
Crystal size	0.180 x 0.160 x 0.050 mm^3	
Theta range for data collection	3.597 to 73.045°.	
Index ranges	-6<=h<=6, -29<=k<=26, -17<=l<=17	
Reflections collected	29409	
Independent reflections	7096 [R(int) = 0.0341]	
Completeness to theta = 67.684°	100.0 %	
Absorption correction	Semi-empirical from equivalents	

Max. and min. transmission	1.00000 and 0.88357
Refinement method	Full-matrix least-squares on F^2
Data / restraints / parameters	7096 / 1 / 527
Goodness-of-fit on F^2	1.011
Final R indices [I>2sigma(I)]	R1 = 0.0318, wR2 = 0.0795
R indices (all data)	R1 = 0.0343, wR2 = 0.0809
Absolute structure parameter	-0.010(7)
Extinction coefficient	n/a
Largest diff. peak and hole	0.473 and -0.293 e.$Å^{-3}$
CCDC	2253111

5.3 FTIR spectrum of C1

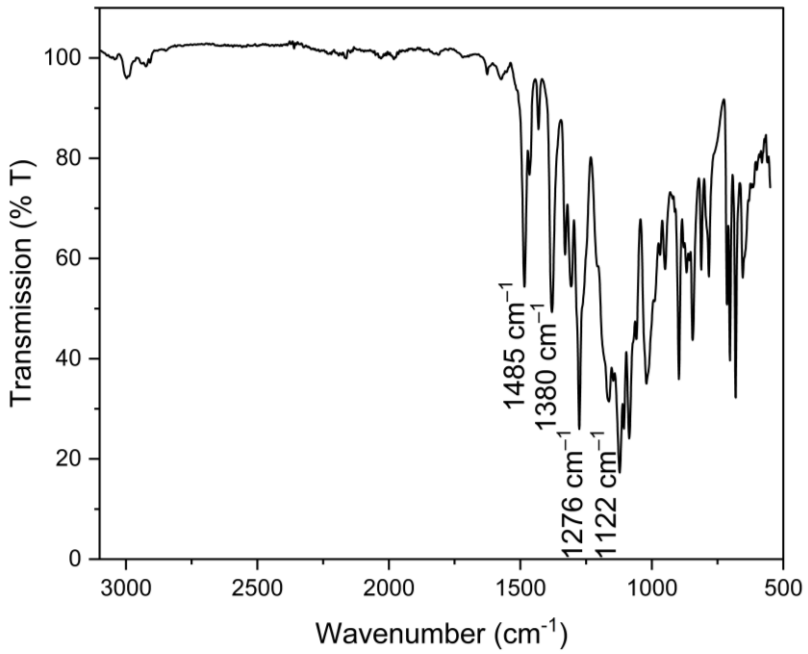

Fig. S22 FTIR spectrum of **C1**.

6 Characterisation of Poly(D-Ox-*alt*-ITCX)

6.1 NMR analysis of poly(D-Ox-*alt*-ITC4)

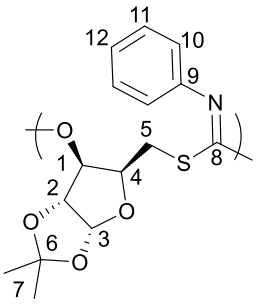

^{1}H NMR (500 MHz, $CDCl_3$) δ (ppm): 7.19 (m, 2H, H−10), 6.99 (m, 1H, H−12), 6.73 (m, 2H, H−11), 5.81 (m, 1H, H−3), 5.54 (m, 1H, H−1), 4.54 (m, 1H, H−2), 4.30 (m, 1H, H−4), 3.15−2.92 (m, 2H, H−5), 1.36 (m, 3H, H−7), 1.07 (m, 3H, H−7).

^{13}C{^{1}H} NMR (126 MHz, $CDCl_3$) δ (ppm): 155.79 (C−8), 145.95 (C−9), 129.29 (C−10), 124.40 (C−12), 121.34 (C−11), 112.01 (C−6), 104.69 (C−3), 83.40 (C−2), 79.91 (C−1), 79.37 (C−4), 29.32 (C−5), 26.72 (C−7), 26.01 (C−7).

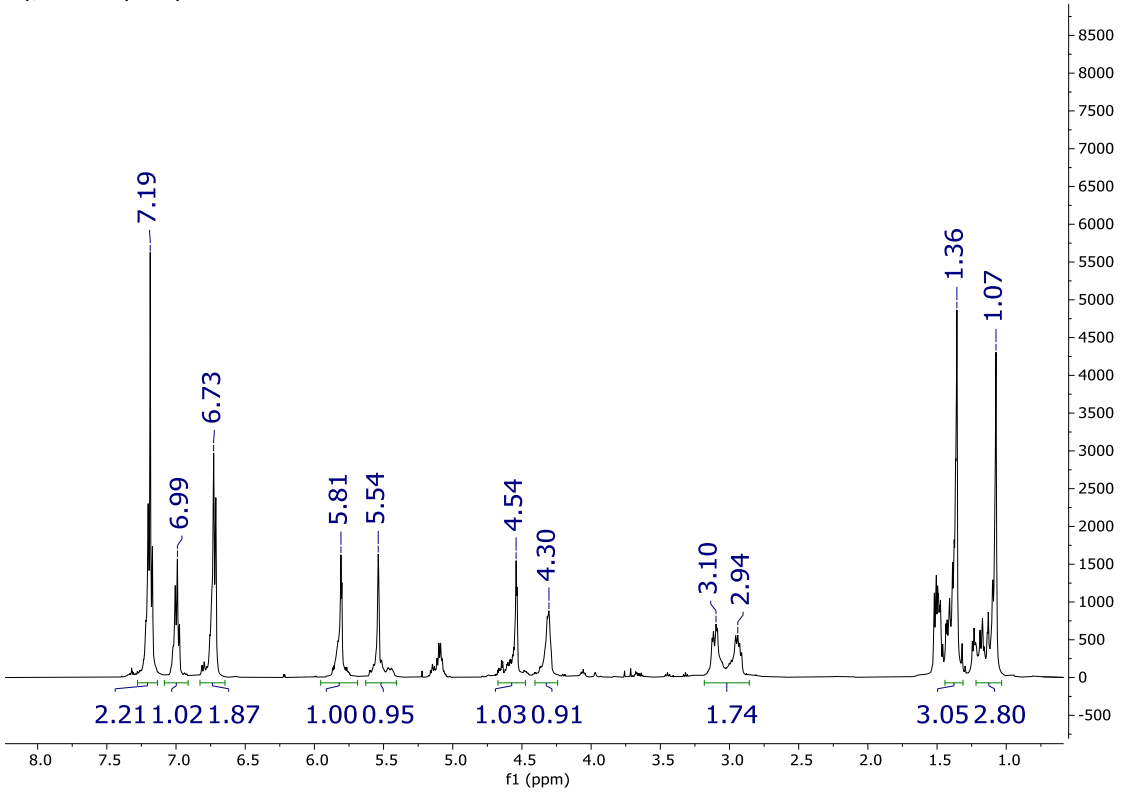

Fig. S23 ^{1}H NMR spectrum ($CDCl_3$) of poly(**D-Ox**-*alt*-**ITC4**) (unidentified peaks at 5.10 and 1.51 ppm).

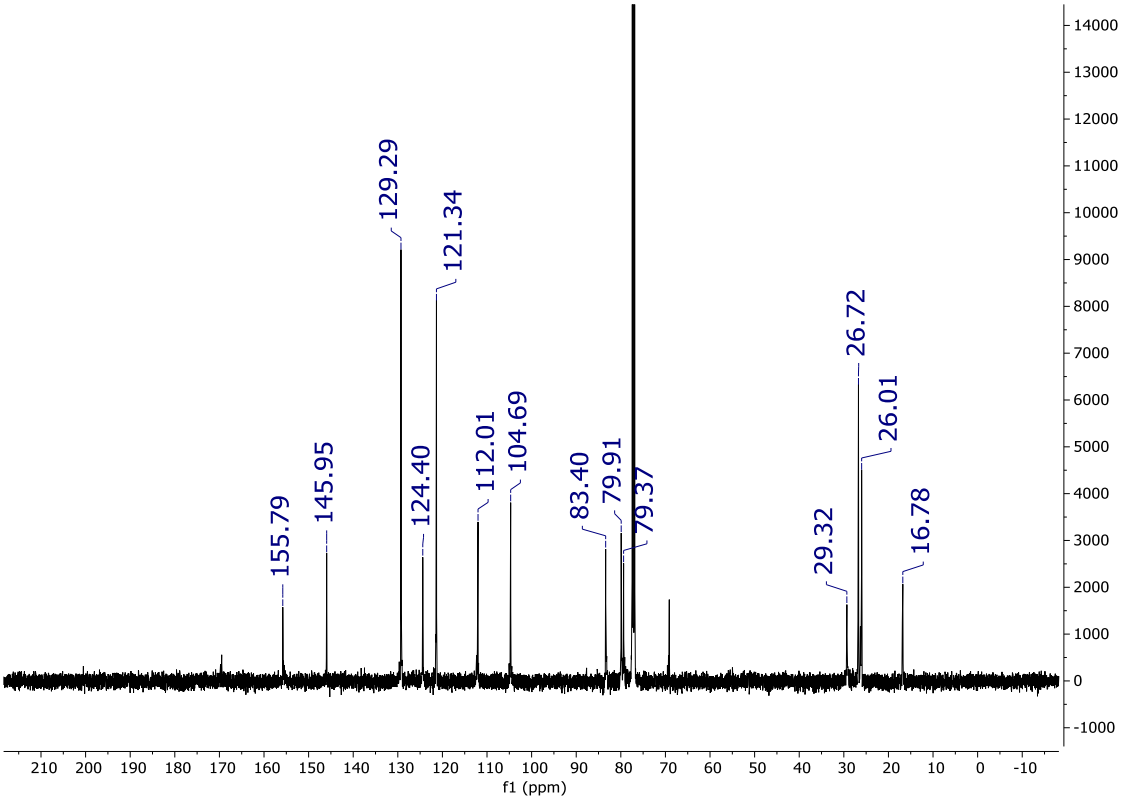

Fig. S24 $^{13}C\{^{1}H\}$ NMR spectrum ($CDCl_3$) of poly(**D-Ox**-*alt*-**ITC4**) (residual $CHCl_3$ peak at 77.16 ppm)

6.2 NMR analysis of poly(D-Ox-*alt*-ITC5)

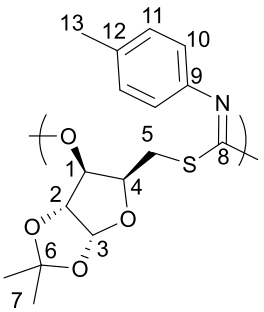

^{1}H NMR (500 MHz, $CDCl_3$) δ (ppm): 7.06 (m, 2H, H−19, H−10), 6.69 (m, 2H, H−11), 5.86 (m, 1H, H−3), 5.60 (m, 1H, H−1), 4.60 (m, 1H, H−2), 4.37 (m, 1H, H−4), 3.20−2.94 (m, 2H, H−5), 2.29 (m, 3H, H−13), 1.42 (m, 3H, H−7), 1.14 (m, 3H, H−7).

$^{13}C\{^{1}H\}$ NMR (126 MHz, $CDCl_3$) δ (ppm): 155.62 (C−8), 143.39 (C−9), 133.77 (C−12), 129.86 (C−11), 121.17 (C−10), 111.96 (C−6), 104.71 (C−3), 83.44 (C−2), 79.85 (C−1), 79.49 (C−4), 29.37 (C−5), 26.73 (C−7), 25.97 (C−7), 21.04 (C−13).

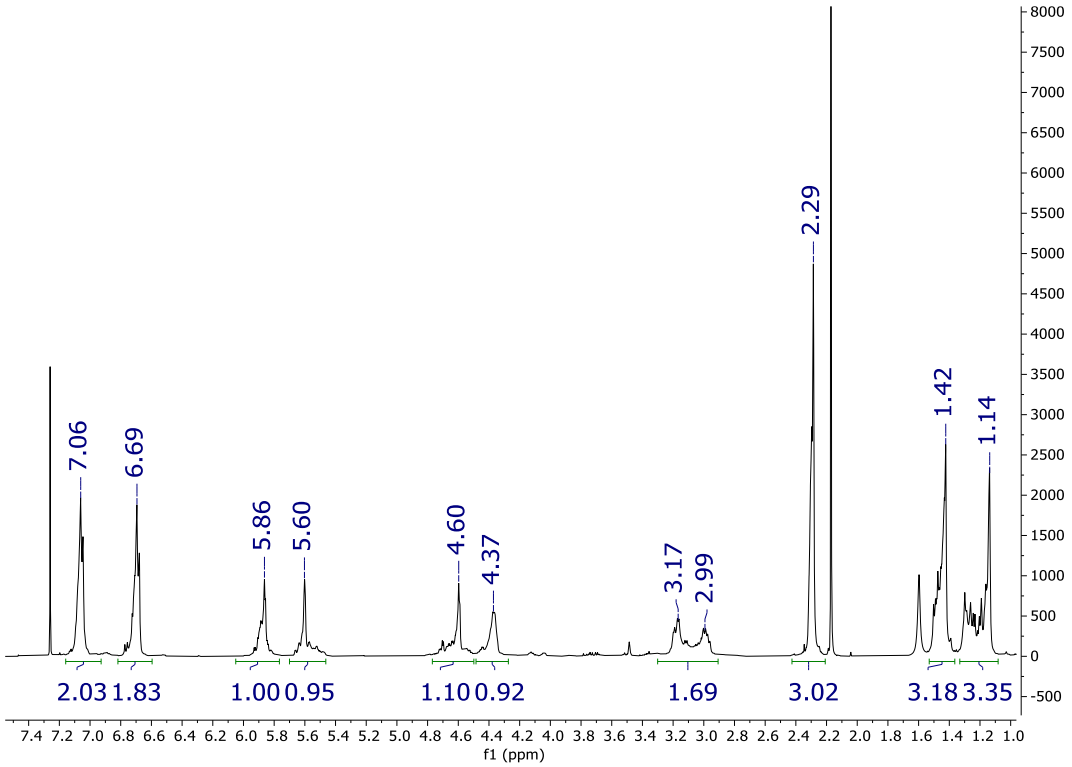

Fig. S25 ^{1}H NMR spectrum ($CDCl_3$) of poly(**D -Ox**-*alt*-**ITC5**)($CHCl_3$, acetone and water residual signal at 7.26, 2.17 and 1.56 ppm respectively).

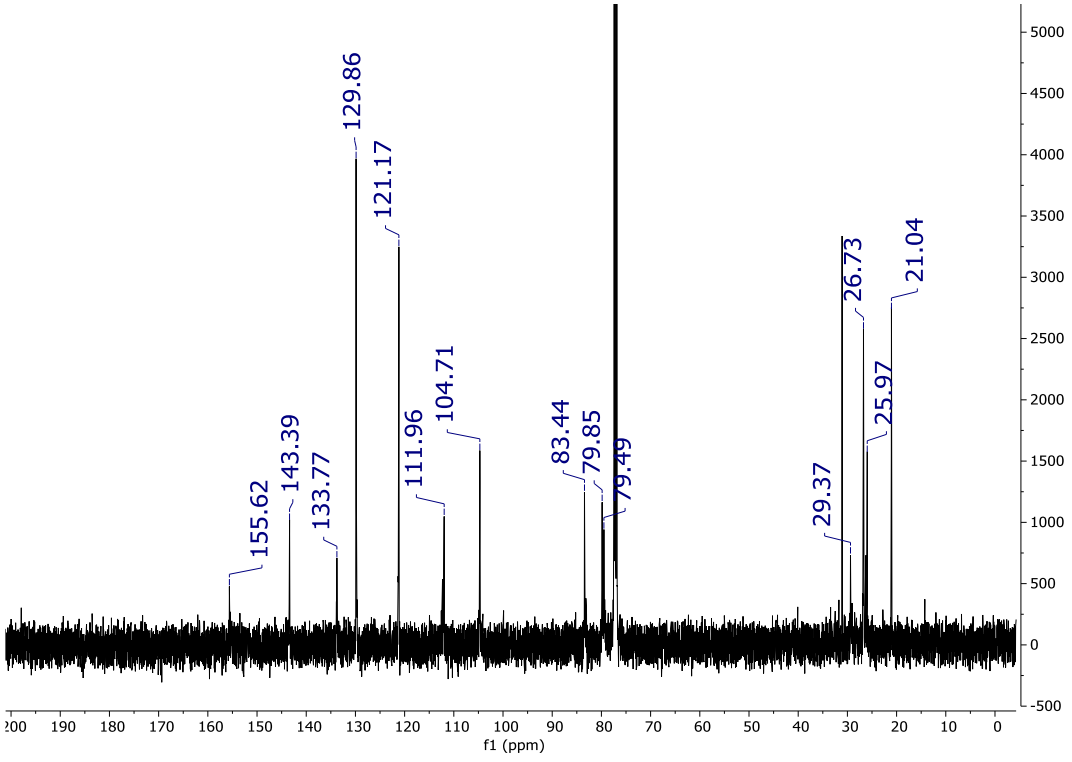

Fig. S26 $^{13}C\{^{1}H\}$ NMR spectrum ($CDCl_3$)of poly(**D-Ox**-*alt*-**ITC5**) ($CHCl_3$ and acetone residual signal at 207.07, 77.16 and 30.92 ppm respectively).

6.3 Thermal analysis of poly(D-Ox-*alt*-ITCX)

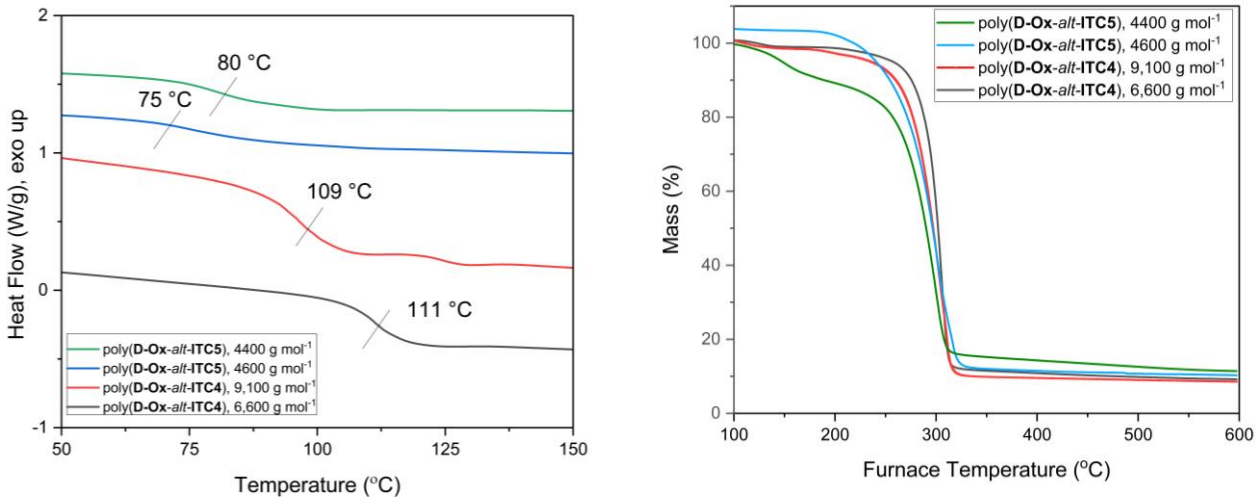

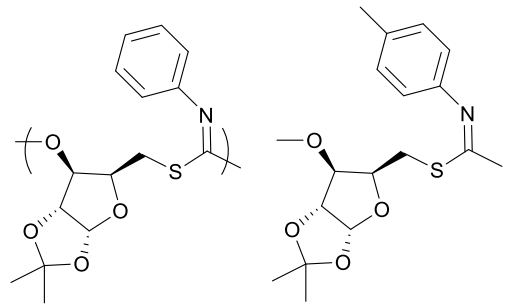

Poly(**D-Ox**-*alt*-**ITC4**) Poly(**D-Ox**-*alt*-**ITC5**)

Fig. S27 Left, plot showing the second heating cycle traces obtained from the DSC thermograms of poly(**ITC4**-*alt*- **D-Ox**) and poly(**ITC5**-*alt*-**D-Ox**) (traces are y−offset and zoomed into T_g region for clarity). Right, remaining mass % vs furnace temperature of poly(**ITC4**-*alt*-**D-Ox**) and poly(**ITC5**-*alt*-**D-Ox**) (Data presented in Table 2).

6.4 NMR analysis of crosslinked polymers

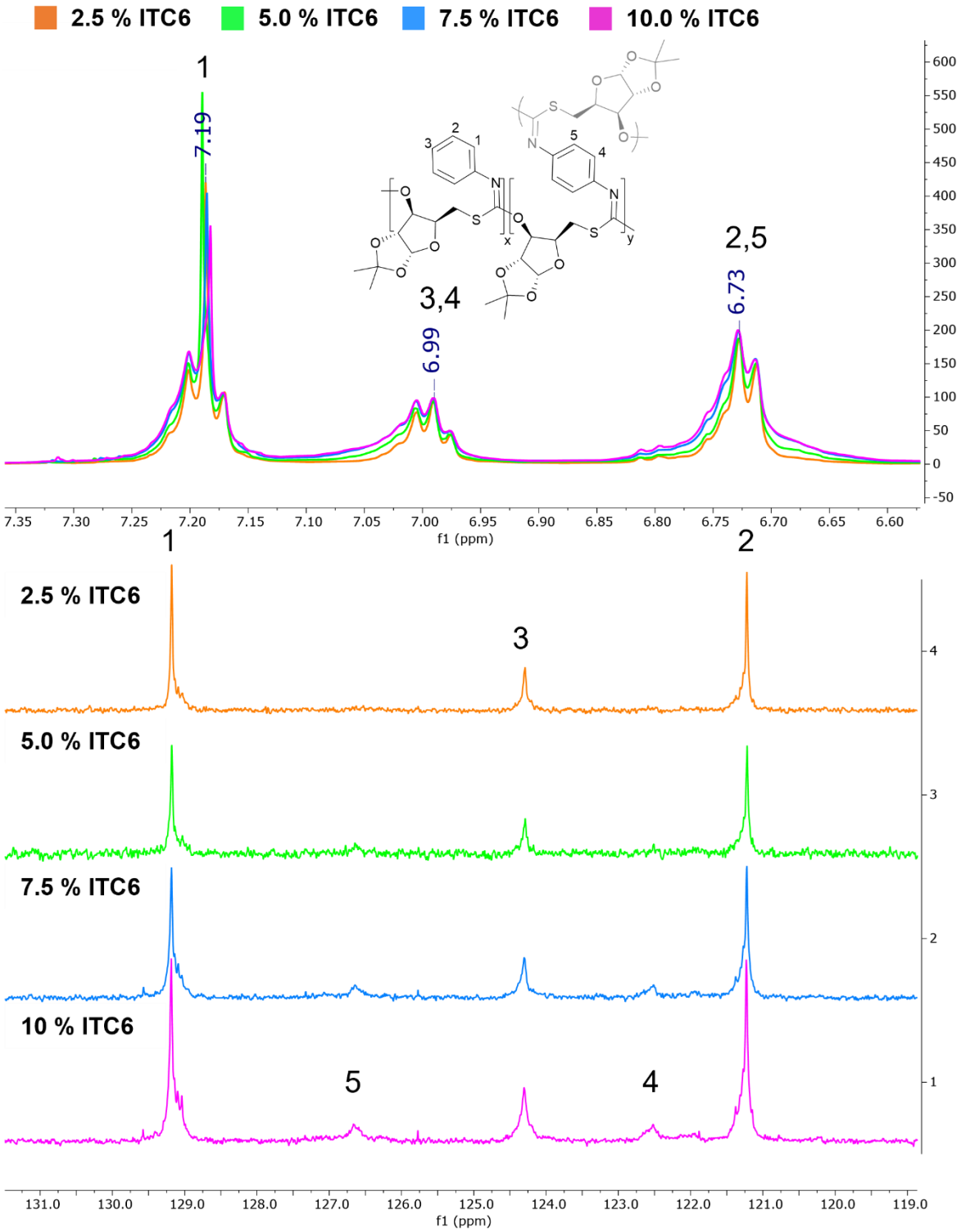

Fig. S28 NMR analysis ($CDCl_3$) varying **ITC6** % in poly(**D-Ox**-*alt*-**ITC4**)$_x$(**D-Ox**-*alt*-**ITC6**)$_y$. Top: overlayed ^{1}H NMR spectrum zoomed into the aromatic region between 7.35 – 6.60 ppm. Bottom: stacked ^{13}C{H} NMR spectrum zoomed into the aromatic region between 131.0 – 119.0 ppm.

6.5 Thermal analysis of crosslinked polymers

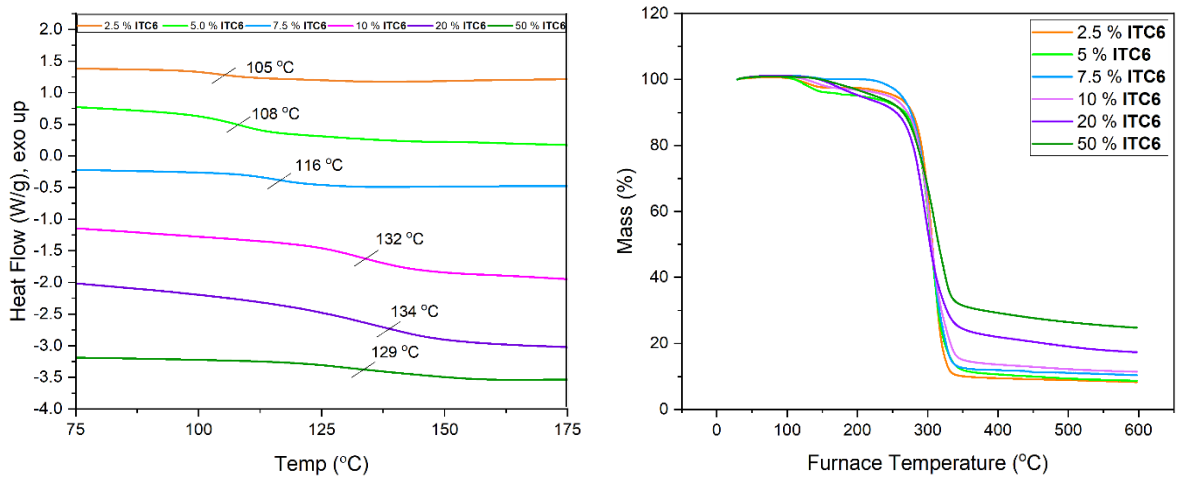

Fig. S29 Left, plot showing the second heating cycle traces obtained from the DSC thermograms of crosslinked polymers (traces are y−offset and zoomed into T_g region for clarity). Right, remaining mass % vs furnace temperature of crosslinked polymers (Data presented in Table 2).

7 Degradation

7.1 NMR analysis of acid degradation products

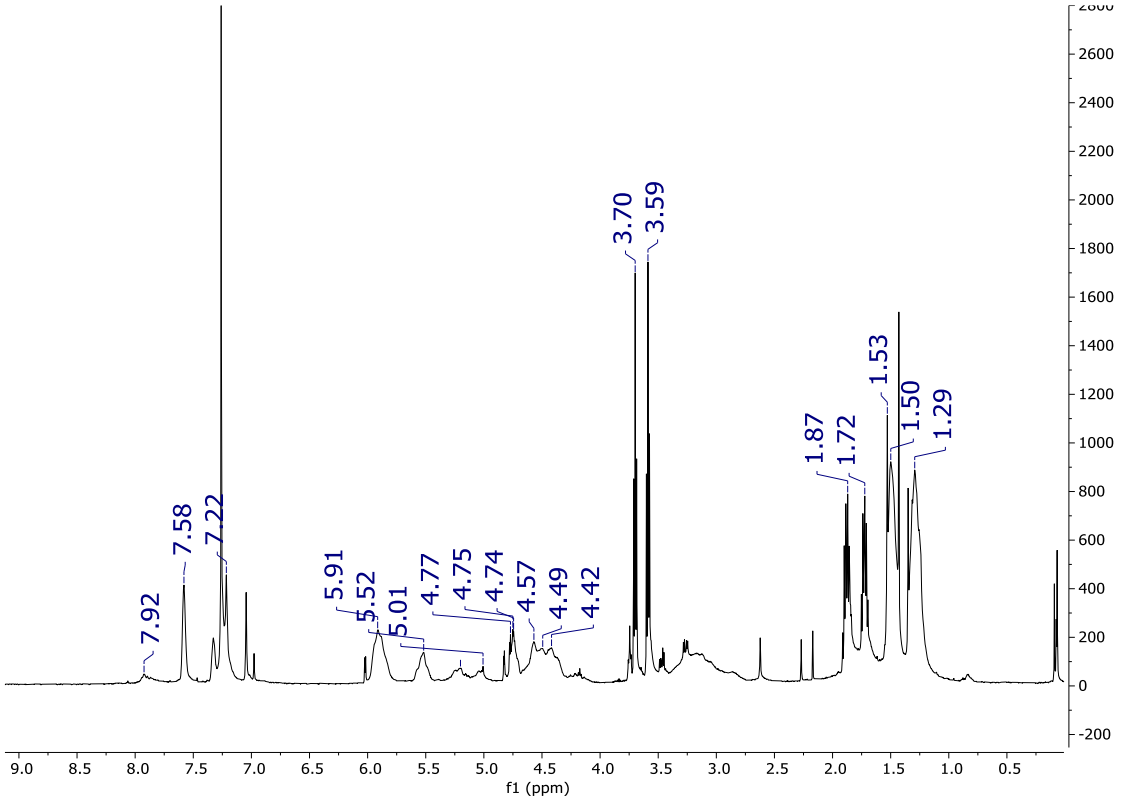

Fig. S30 Crude ^{1}H NMR spectrum ($CDCl_3$) of the acid degradation products of poly(**D-Ox**-*alt*-**ITC1**) after three hours ($CHCl_3$ residual signal at 7.26 ppm).

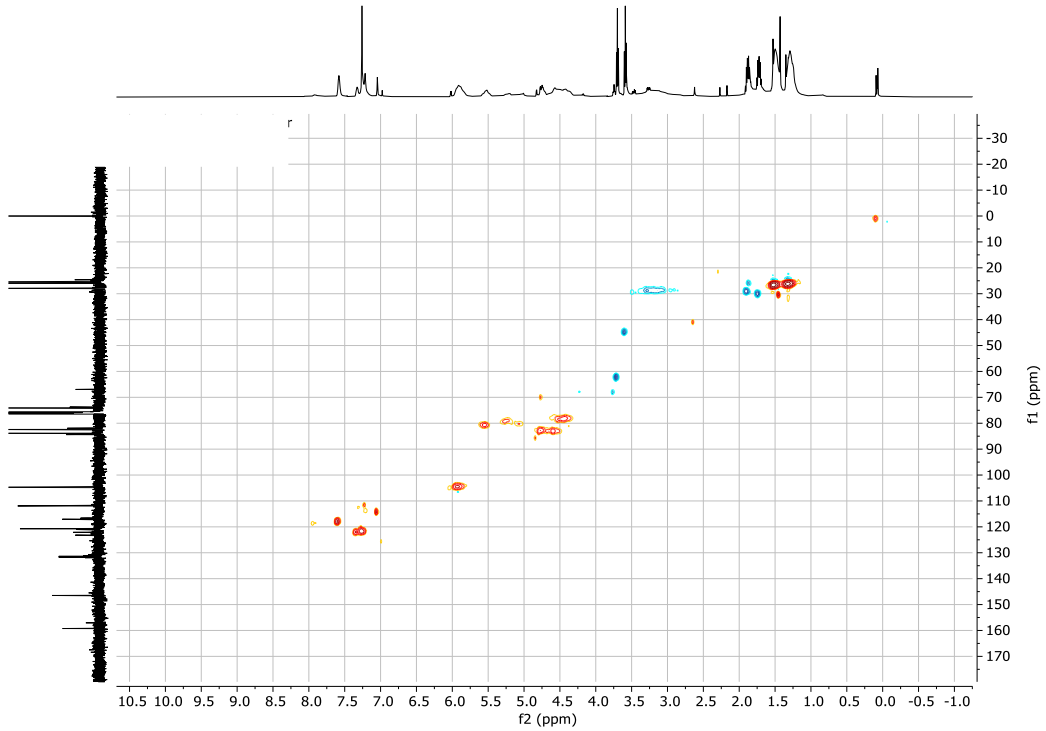

Fig. S31 Crude ^{1}H-$^{13}C\{^{1}H\}$ HSQC NMR spectrum ($CDCl_3$) of the acid degradation products of poly(**D-Ox**-*alt*-**ITC1**) after three hours.

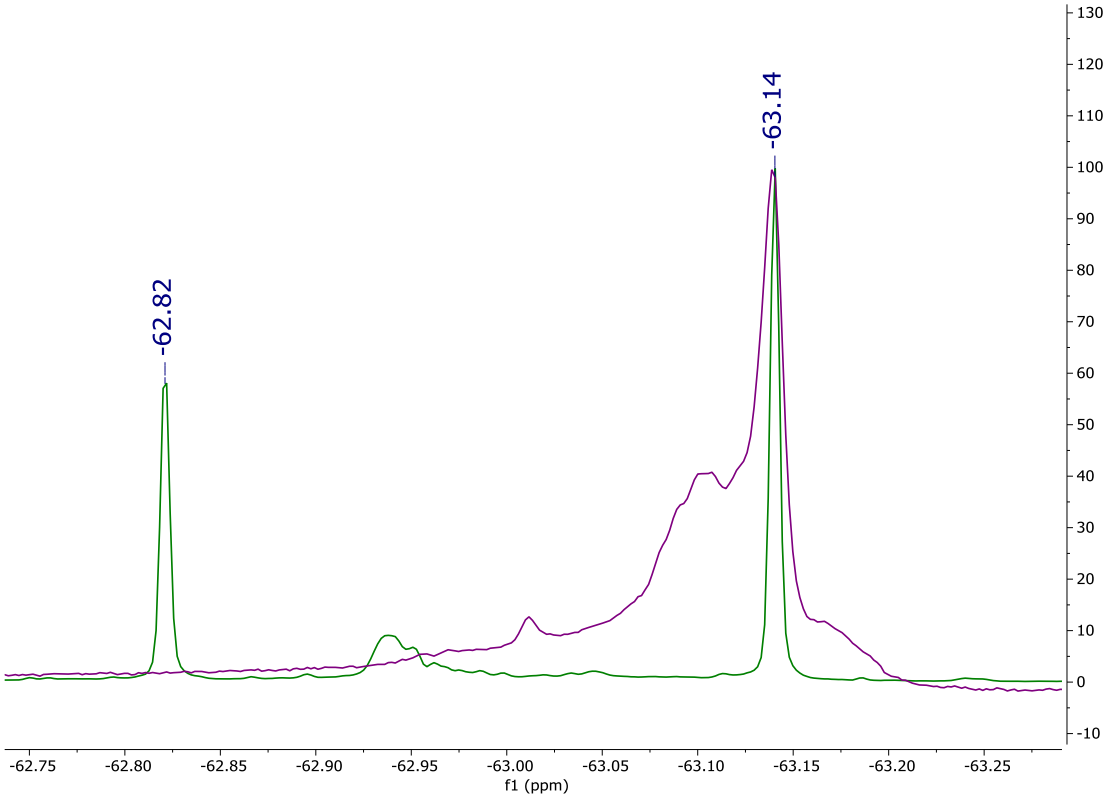

Fig. S32 Superimposed ^{19}F NMR spectra ($CDCl_3$) of poly(**D-Ox**-*alt*-**ITC1**) (purple) and the product of its acid degradation after three hours (green).

7.2 NMR analysis of basic degradation products

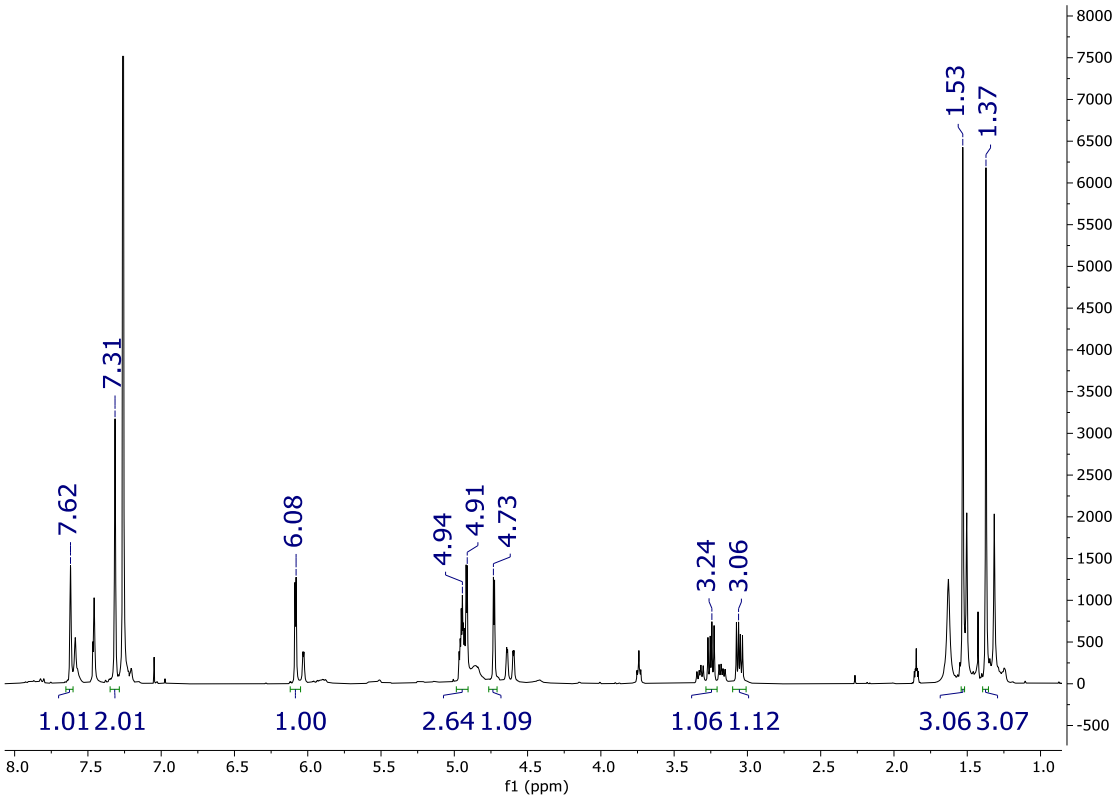

Fig. S33 Crude ^1H NMR spectrum ($CDCl_3$) of the basic degradation products of poly(**D-Ox**-*alt*-**ITC1**) after 1 hour ($CHCl_3$ residual signal at 7.26 ppm).

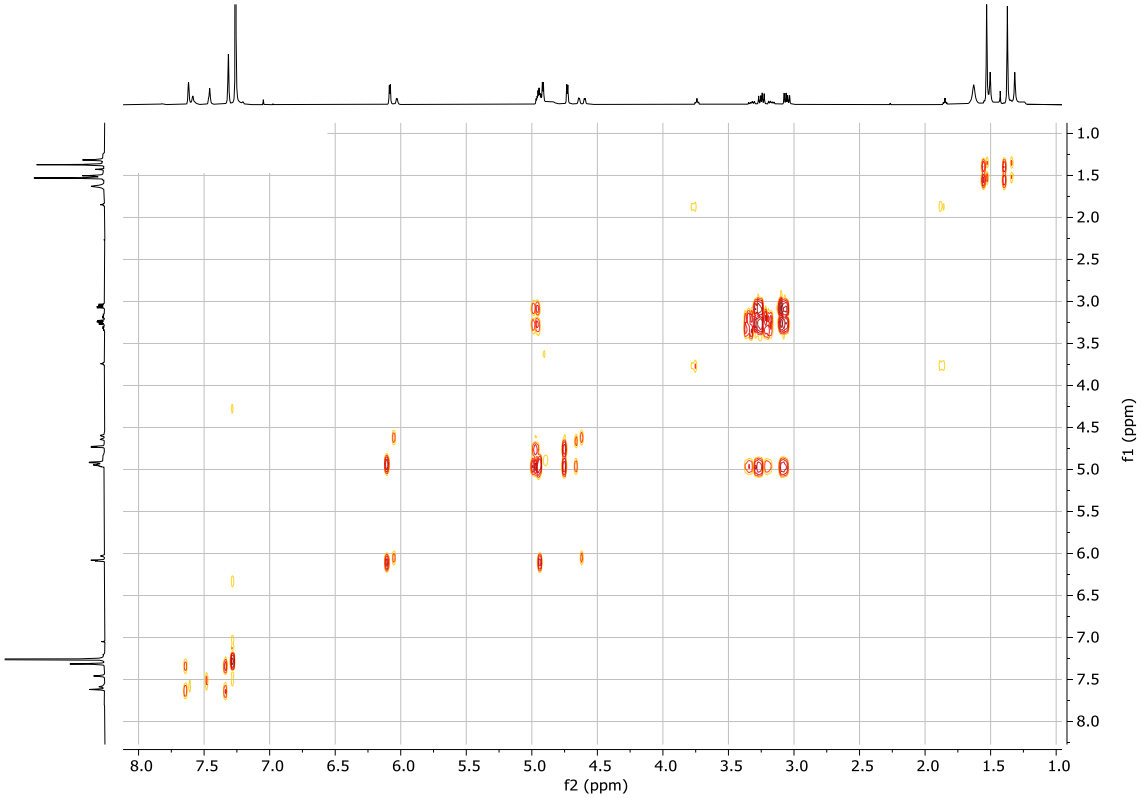

Fig. S34 Crude ^{1}H COSY NMR spectrum ($CDCl_3$) of the basic degradation products of poly(**D-Ox**-*alt*-**ITC1**) after 1 hour.

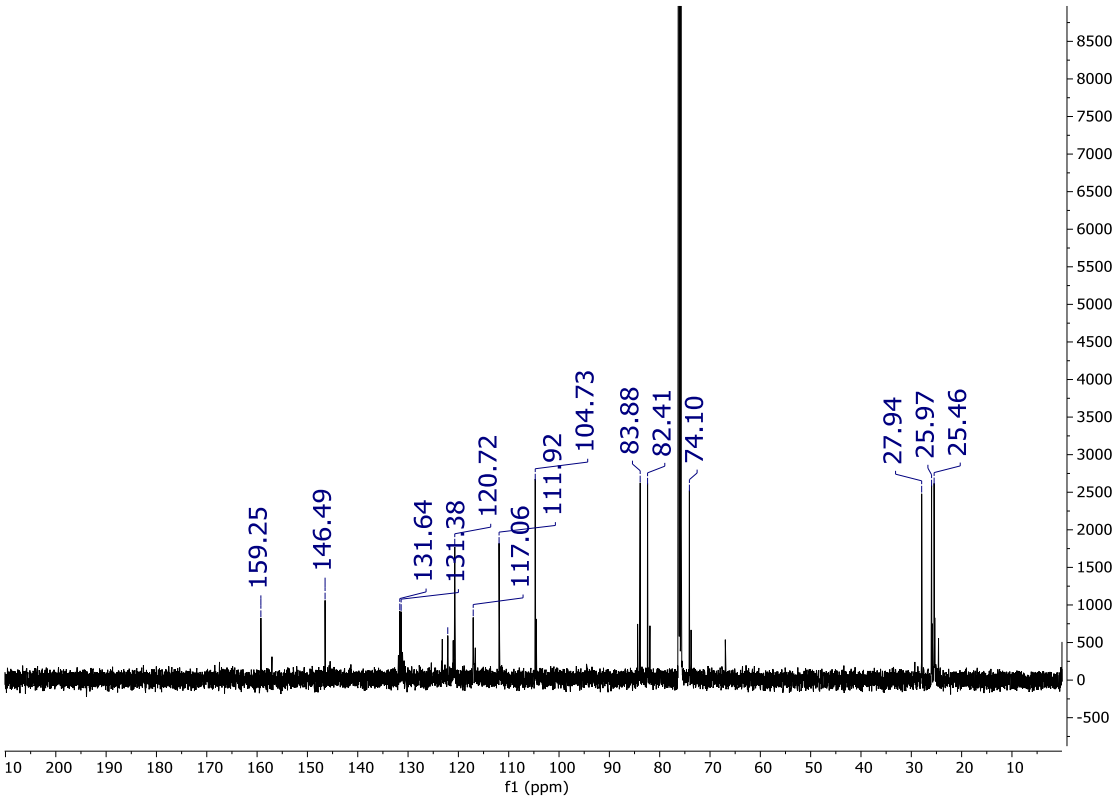

Fig. S35 Crude ^{13}C{H} NMR spectrum of the basic degradation products of poly(**D-Ox**-*alt*-**ITC1**) after 1 hour ($CHCl_3$ residual signal at 77.16 ppm).

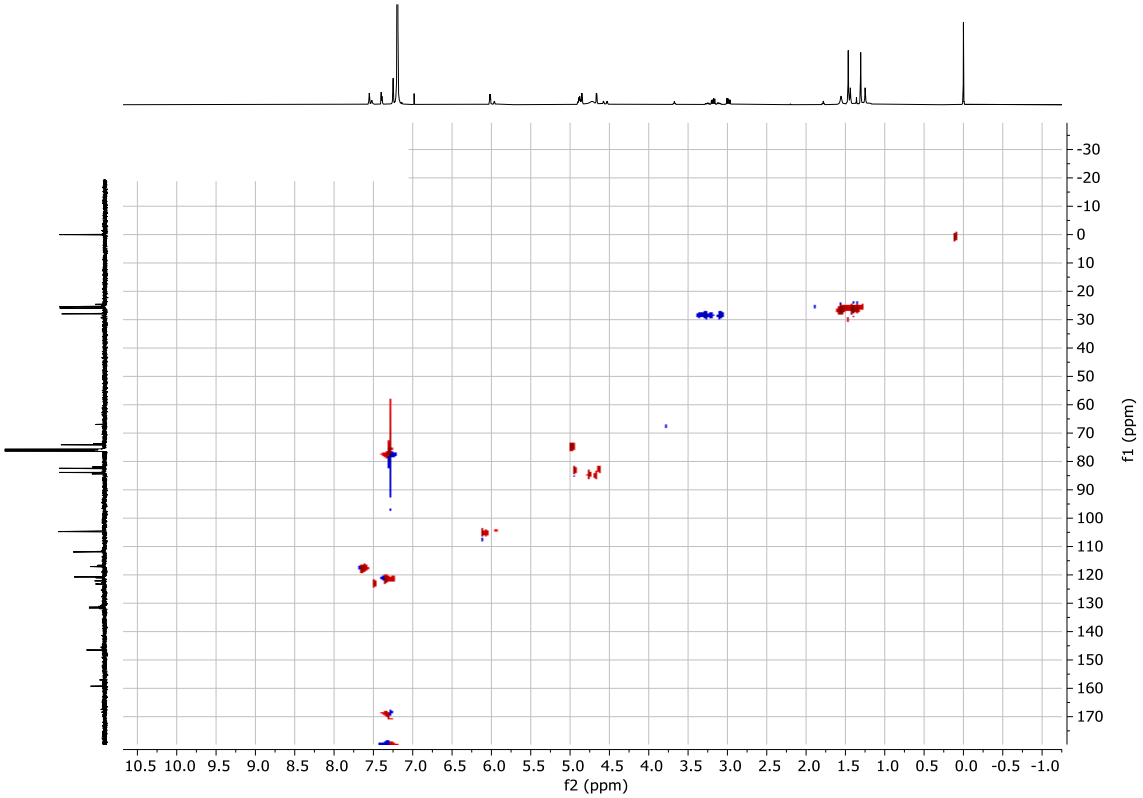

Fig. S36 Crude ^{1}H-$^{13}C\{^{1}H\}$ HSQC NMR spectrum ($CDCl_3$) of the basic degradation products of poly(**D-Ox**-*alt*-**ITC1**) after 1 hour.

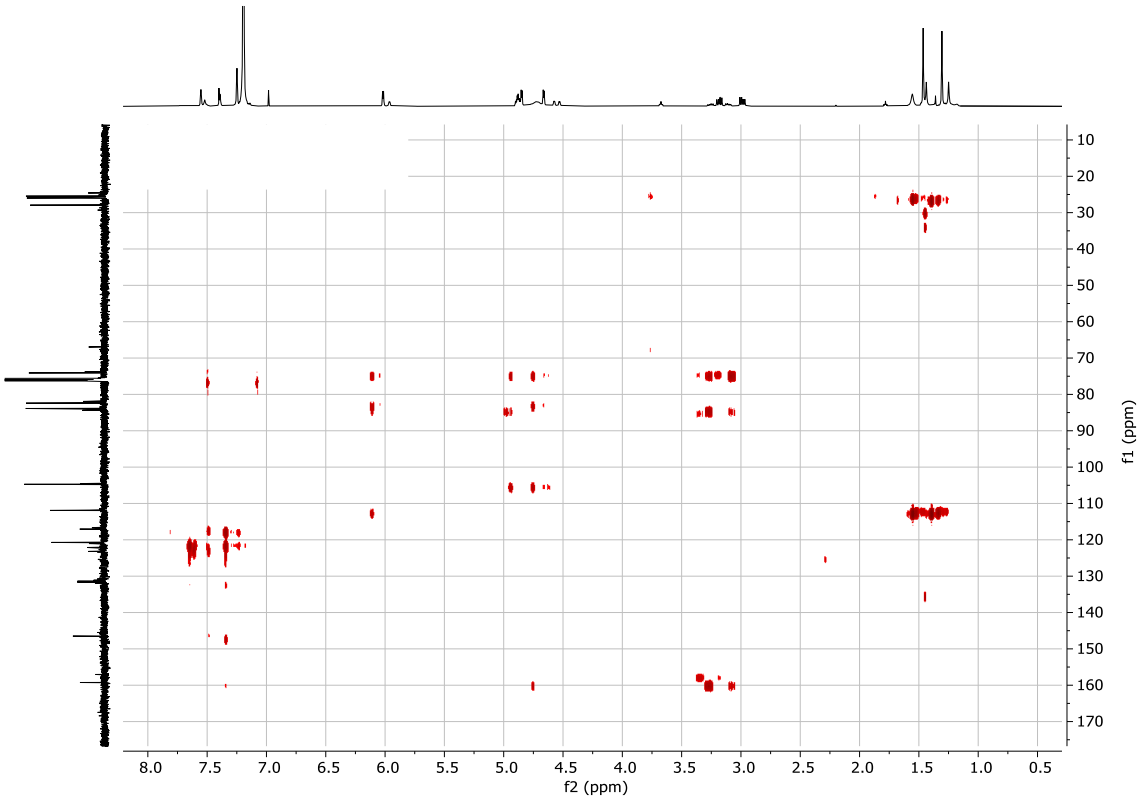

Fig. S37 Crude ^{1}H-$^{13}C\{^{1}H\}$ HMBC NMR spectrum ($CDCl_3$) of the basic degradation of poly(**D-Ox**-*alt*-**ITC1**) after 1 hour.

7.3 Mass spectrometry analysis of basic degradation products

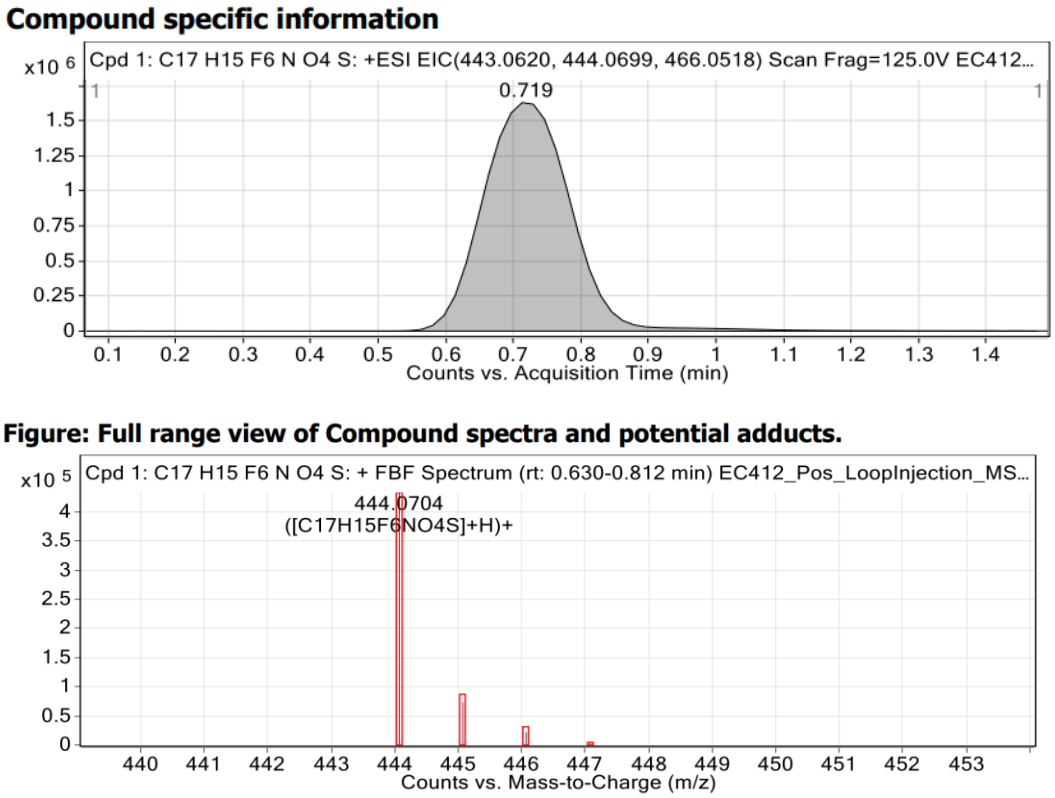

Fig. S38 Mass spectrometry analysis of the basic degradation of poly(**D-Ox**-*alt*-**ITC1**) after 1 hour. Top: extracted ion chromatogram for $C_{17}H_{15}F_6NO_4S$. Bottom: predicted isotope pattern (red) against found isotope pattern (black) for $C_{17}H_{15}F_6NO_4S$.

7.4 NMR analysis of UV degradation products

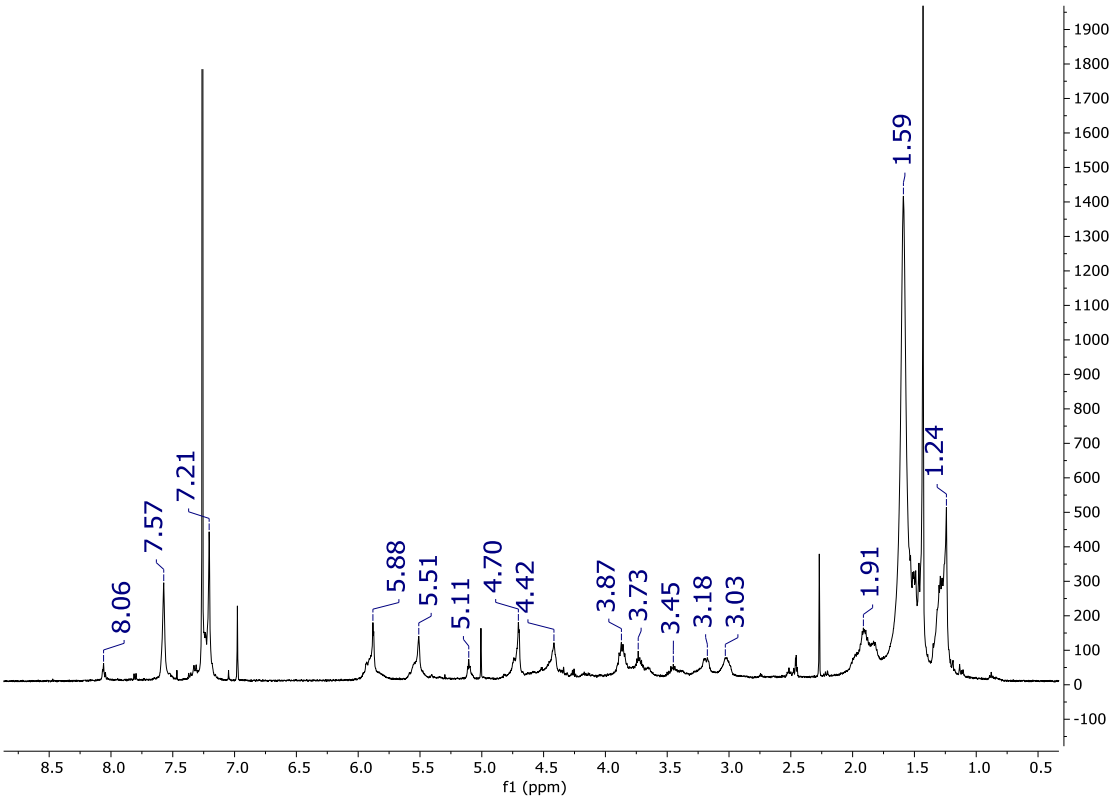

Fig. S39 Crude ^{1}H NMR spectrum ($CDCl_3$) of the photodegradation products of poly(**D-Ox**-*alt*-**ITC1**) after 1 week under 365 nm radiation ($CHCl_3$ residual signal at 7.26 ppm).

8 Microstructure Variations

8.1 Table of initiation of D-Ox/ITC1 with 1,4-butanediol

Table S2 Initiation of **D-Ox**/**ITC1** with 1,4-butanediol

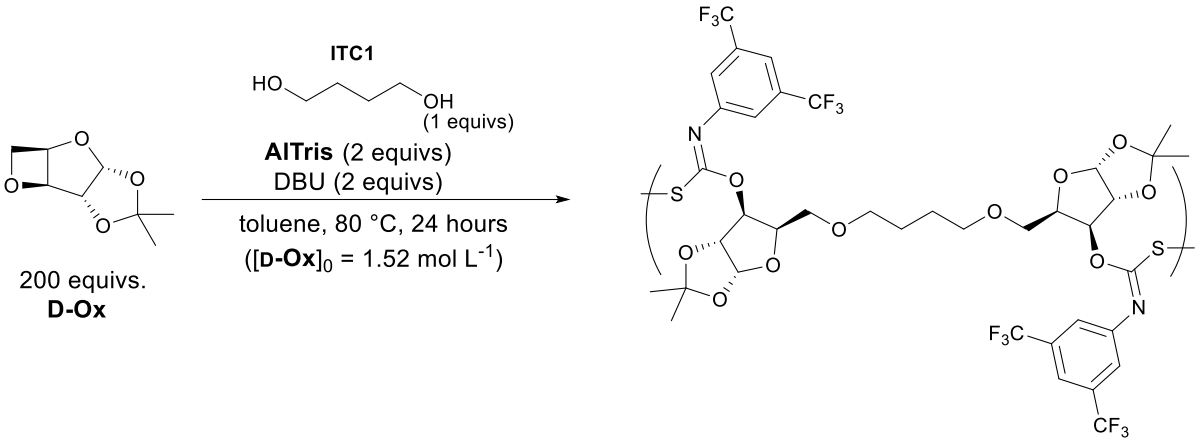

Entry	BD:**D-Ox**	Conv (%)[a]	Select (%)[b]	$M_{n,theo}$[c]	$M_{n,SEC}$[d] ($Đ_M$)
1	1:40	>99	70	12,500	8,400 (1.20)
2	1:100	>99	87	38,600	9,300 (1.26)
3	1:200	90	92	73,600	11,000 (1.37)
4	1:300	79	92	97,100	11,100 (1.15)
5	1:400	55	91	88,700	8,500 (1.14)

Reactions carried out at [**D-Ox**]$_0$ = 1.52 mol L^{-1} in toluene with a 200:200:1:1 ratio of **D-Ox**:**ITC1**:AlTris:PPNCl unless otherwise stated, reaction quenched when stirring stopped. [a]Conversion of **D-Ox** determined by ^{1}H NMR spectroscopy by relative integration of anomeric protons in **D-Ox** ($CDCl_3$, δ = 6.26 ppm (d, J = 3.7 Hz)), poly(**D-Ox**-*alt*-**ITC1**) ($CDCl_3$, δ = 5.81 ppm (m)) and **1** ($CDCl_3$, δ = 6.14 ppm (d, J = 3.7 Hz)). [b] Percentage of converted **D-Ox** to poly(**D-Ox**-*alt*-**ITC1**). [c]Calculated as M_r(Diol)+(((M_r(**D–Ox**)+M_r(**ITC1**)) × [**D–Ox**]$_0$/[PPNCl]$_0$ × %conv./100). [d]Calculated by SEC relative to polystyrene standards in THF eluent, $Đ_M = M_w/M_n$.

8.2 NMR analysis of 1,4-butanediol-initiated copolymer

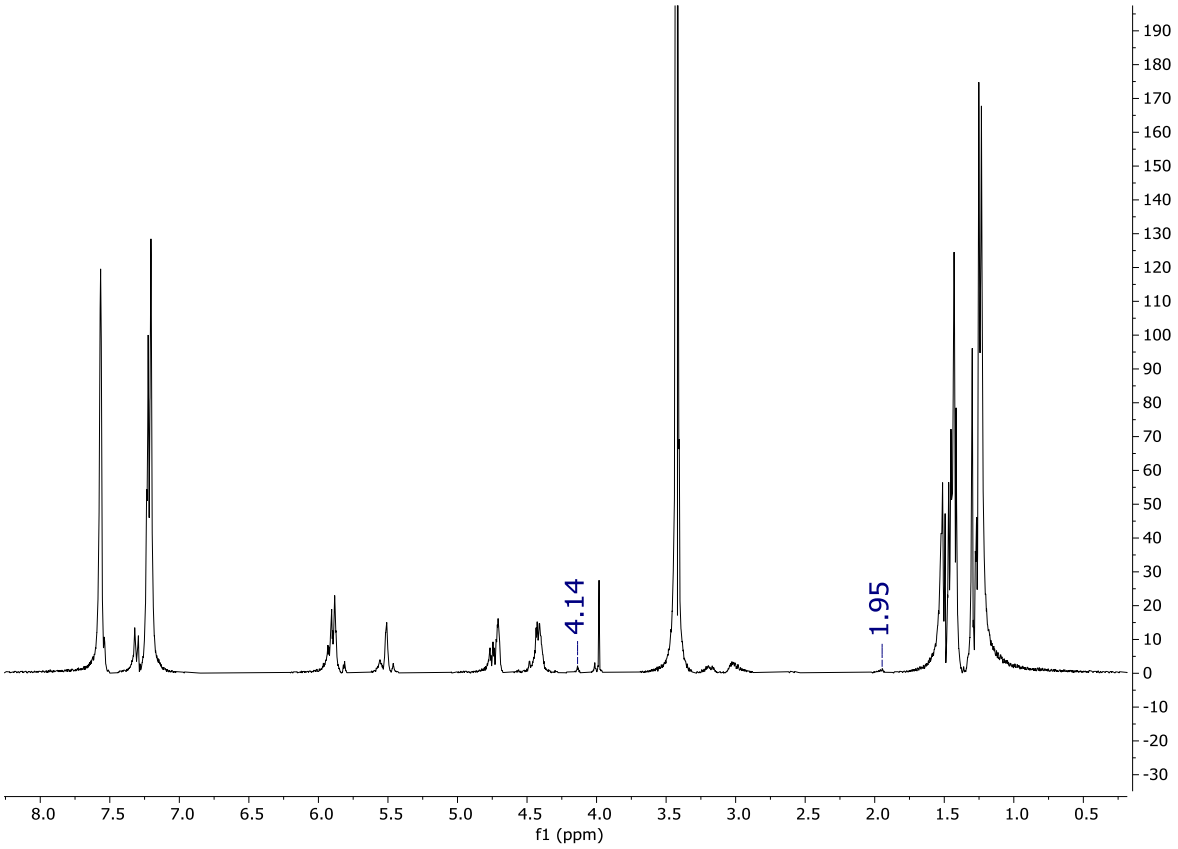

Fig. S40 ^{1}H NMR spectrum ($CDCl_3$) of poly(**D-Ox**-*alt*-**ITC1**) initiated from 1,4-butanediol, signals belonging to incorporated 1,4-butanediol at 4.14 and 1.95 ppm shown (residual methanol peak at 3.49 ppm).

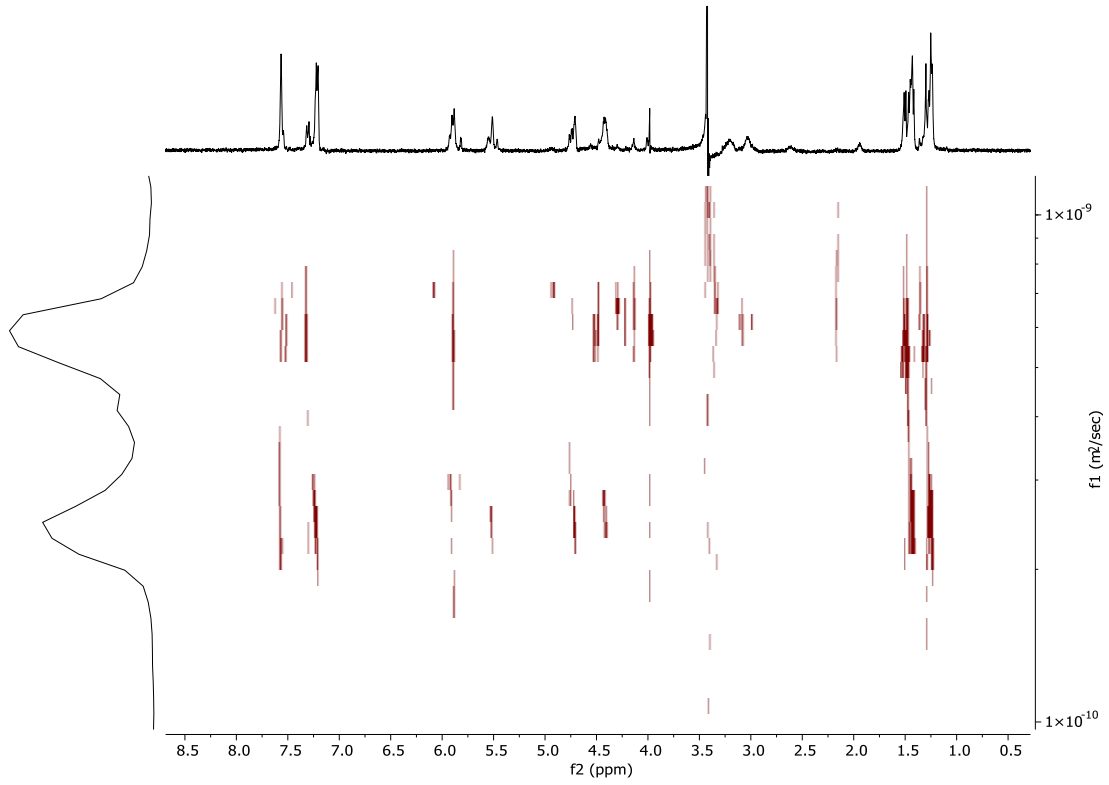

Fig. S41 ^{1}H DOSY NMR spectrum ($CDCl_3$) of poly(**D-Ox**-*alt*-**ITC1**) initiated from 1,4-butanediol.

8.3 MALDI-ToF mass spectrometry analysis of 1,4-butanediol initiated copolymer

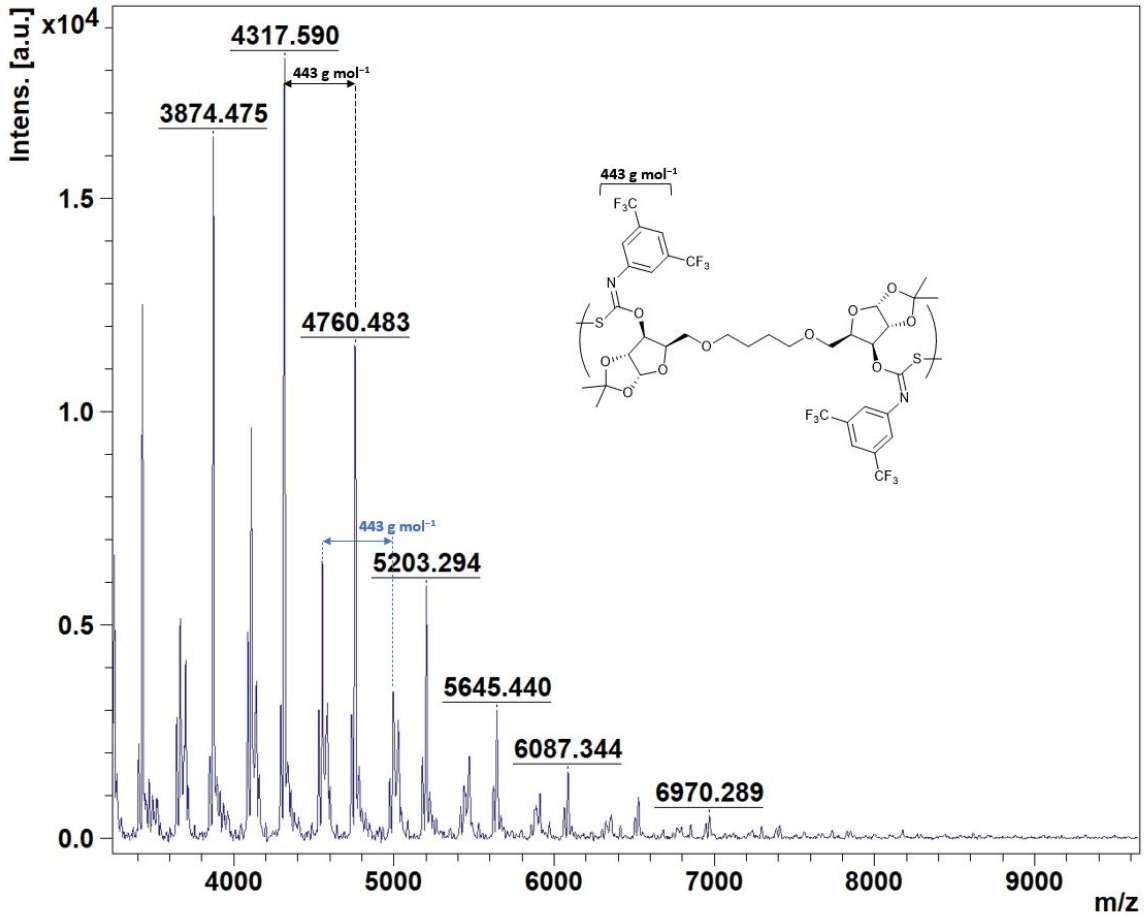

Fig. S42 MALDI-ToF mass spectrum showing detected series for poly(**D-Ox**-*alt*-**ITC1**) initiated from 1,4-butanediol. None of these of these distributions could be clearly identified, expect for their AB repeat unit, which correspond to the **D-Ox** and **ITC1** co-monomers.

8.4 NMR analysis of PEG initiated copolymer

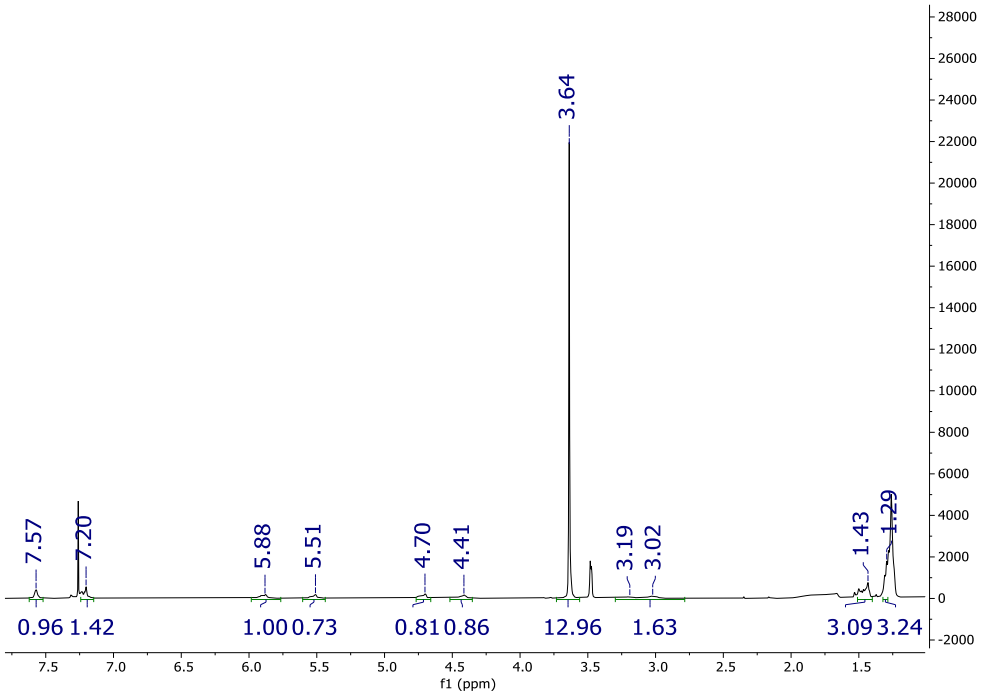

Fig. S43 ^{1}H NMR spectrum ($CDCl_3$) of poly((**D-Ox**-*alt*-**ITC1**)-*b*-PEG-*b*-(**D-Ox**-*alt*-**ITC1**)) (residual $CHCl_3$ and EtO_2 peak at 7.26, 3.48 and 1.21 ppm).

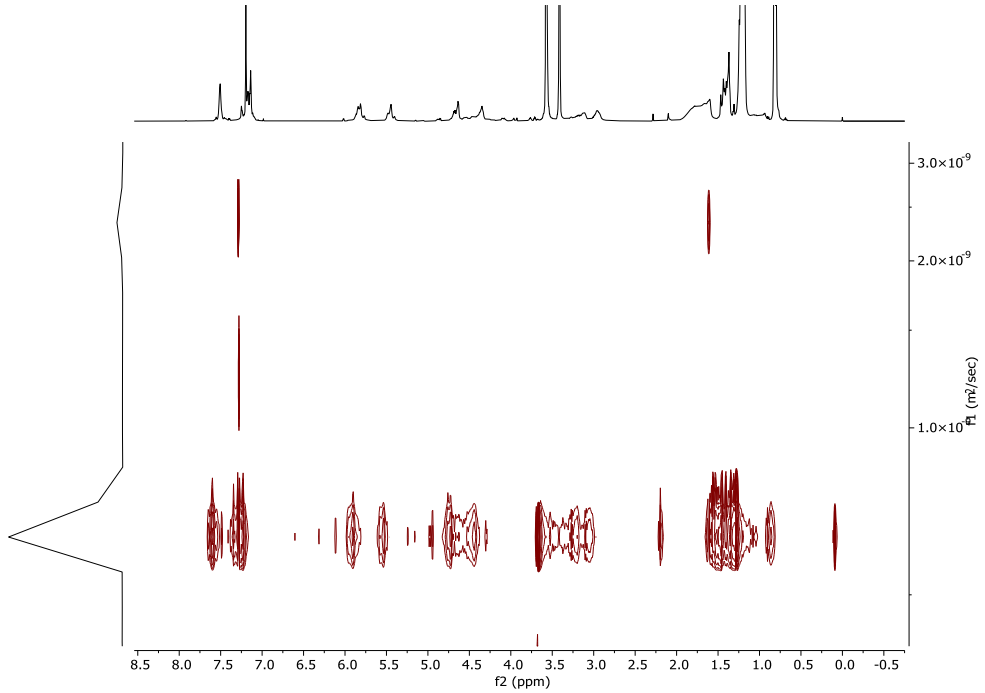

Fig. S44 ^{1}H DOSY NMR spectrum ($CDCl_3$) of poly((**D-Ox**-*alt*-**ITC1**)-*b*-PEG-*b*-(**D-Ox**-*alt*-**ITC1**)) (residual $CHCl_3$ peak at 7.26 ppm).

8.5 Thermal analysis of PEG initiated copolymer

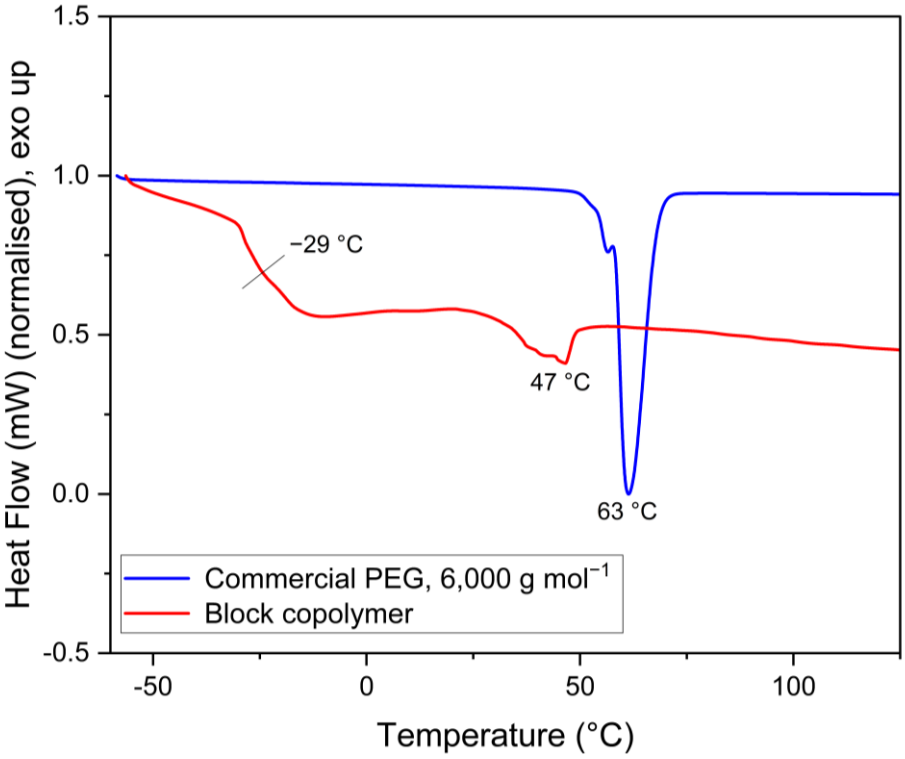

Fig. S45 DSC trace of poly((D-**Ox**-*alt*-**ITC1**)-*b*-PEG-*b*-(D-**Ox**-*alt*-**ITC1**)) (red) and PEG (blue) (second heating cycle).

8.6 NMR analysis of poly(LLA-*b*-(D-Ox-*alt*-ITC1)-*b*-LLA).

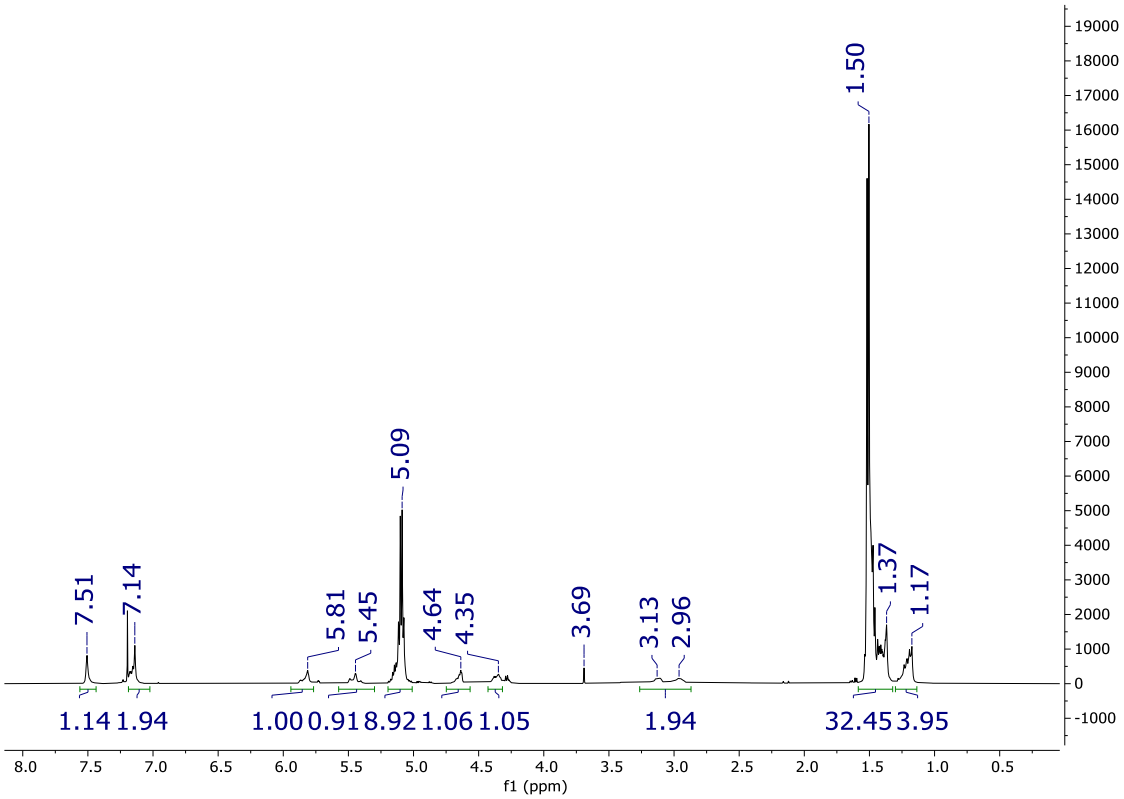

Fig. S46 ^{1}H NMR spectrum ($CDCl_3$) of poly(LLA-*b*-(D-**Ox**-*alt*-**ITC1**)-*b*-LLA) (residual $CHCl_3$ peak at 7.26 ppm).

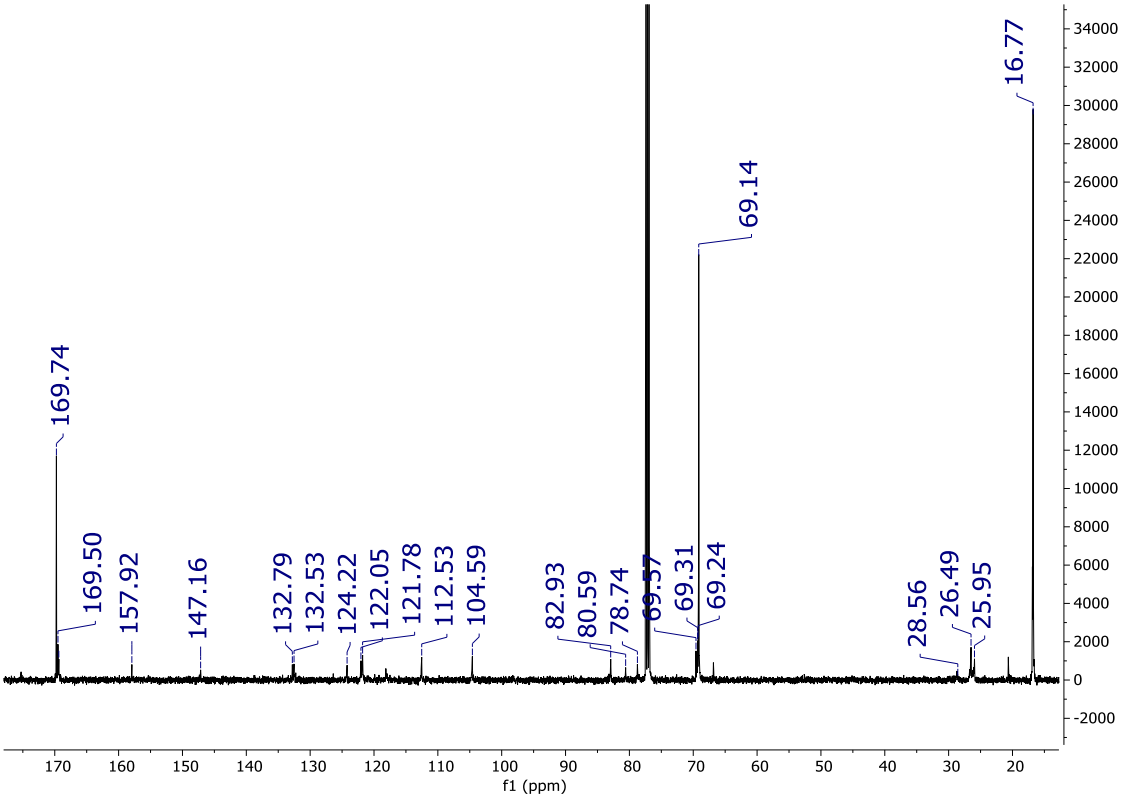

Fig. S47 $^{13}C\{^{1}H\}$ NMR spectrum ($CDCl_3$) of poly(LLA-*b*-(**D-Ox**-*alt*-**ITC1**)-*b*-LLA) (residual $CHCl_3$ peak at 77.16 ppm).

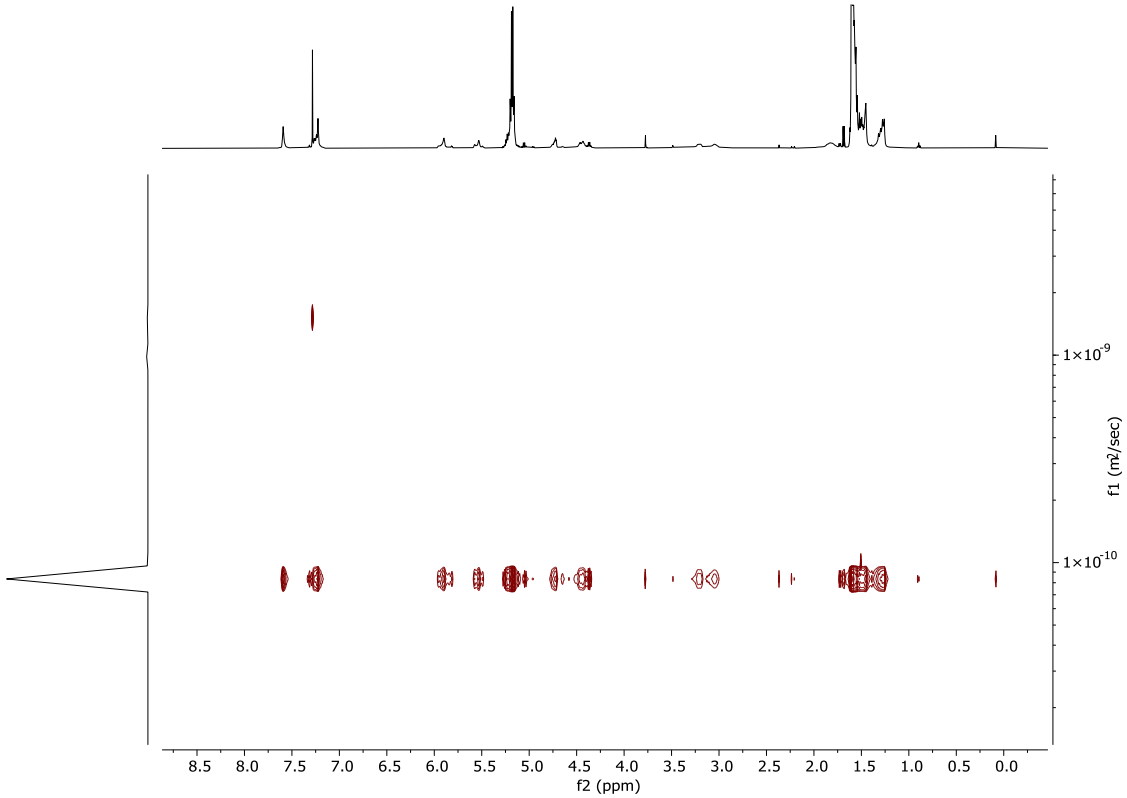

Fig. S48 ^{1}H DOSY NMR spectrum ($CDCl_3$) of poly(LLA-*b*-(**D-Ox**-*alt*-**ITC1**)-*b*-LLA) (residual $CHCl_3$ peak at 7.26 ppm).

8.7 Thermal analysis of poly(LLA-*b*-(D-Ox-*alt*-ITC1)-*b*-LLA).

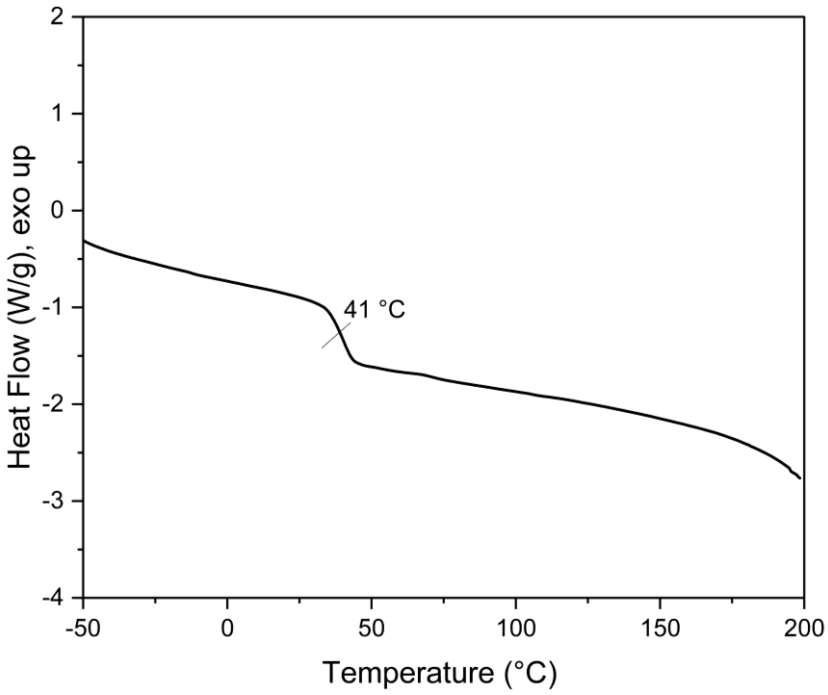

Fig. S49 DSC trace of poly(LLA-*b*-(**D-Ox**-*alt*-**ITC1**)-*b*-LLA) (second heating cycle).

9 Characterisation of Oxathiolane Product

9.1 NMR analysis of (S)-2-((3,5-bis(trifluoromethyl)phenyl)imino)-5-methyl-1,3-oxathiolan-4-one

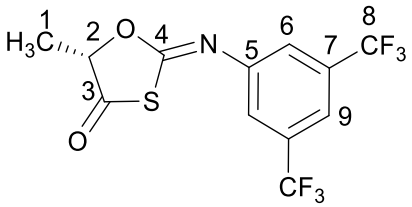

(S)-2-((3,5-bis(trifluoromethyl)phenyl)imino)-5-methyl-1,3-oxathiolan-4-one: white solid; 19 % yield (0.1 g);

^{1}H NMR (500 MHz, $CDCl_3$) δ (ppm): 8.07 (s, 2H, H−6), 7.93 (s, 1H, H−9), 5.09 (q, *J* = 6.9 Hz, 1H, H−2), 1.76 (d, *J* = 7.05 Hz, 3H, H−1).

^{13}C{^{1}H} NMR (126 MHz, $CDCl_3$) δ (ppm): 171.55 (C−3), 152.75 (C−4), 132.94 (C−8), 125.22 (C−6), 123.84 (C−7), 122.54 (C−9), 121.67 (C−5), 76.28 (C−2), 16.90 (C−1).

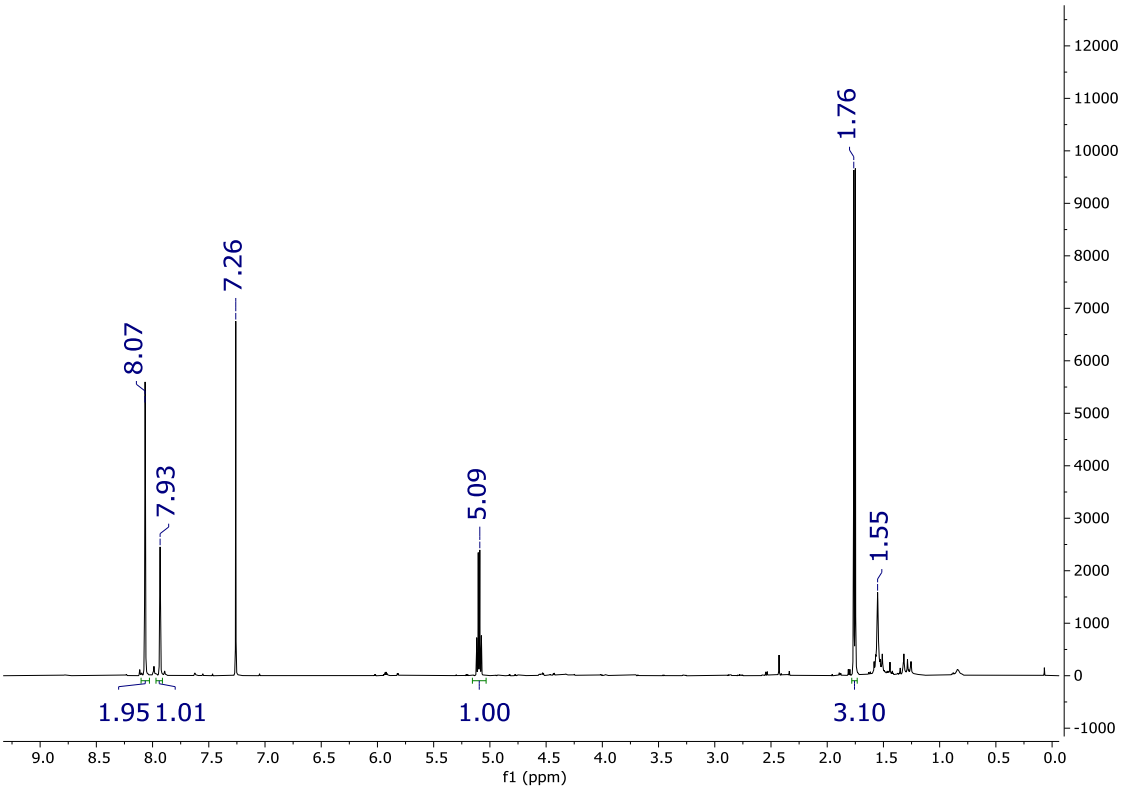

Fig. S50 ^{1}H NMR spectrum ($CDCl_3$) of (S)-2-((3,5-bis(trifluoromethyl)phenyl)imino)-5-methyl-1,3−oxathiolan-4-one (residual chloroform and water peaks at 7.26 and 1.55 respectively).

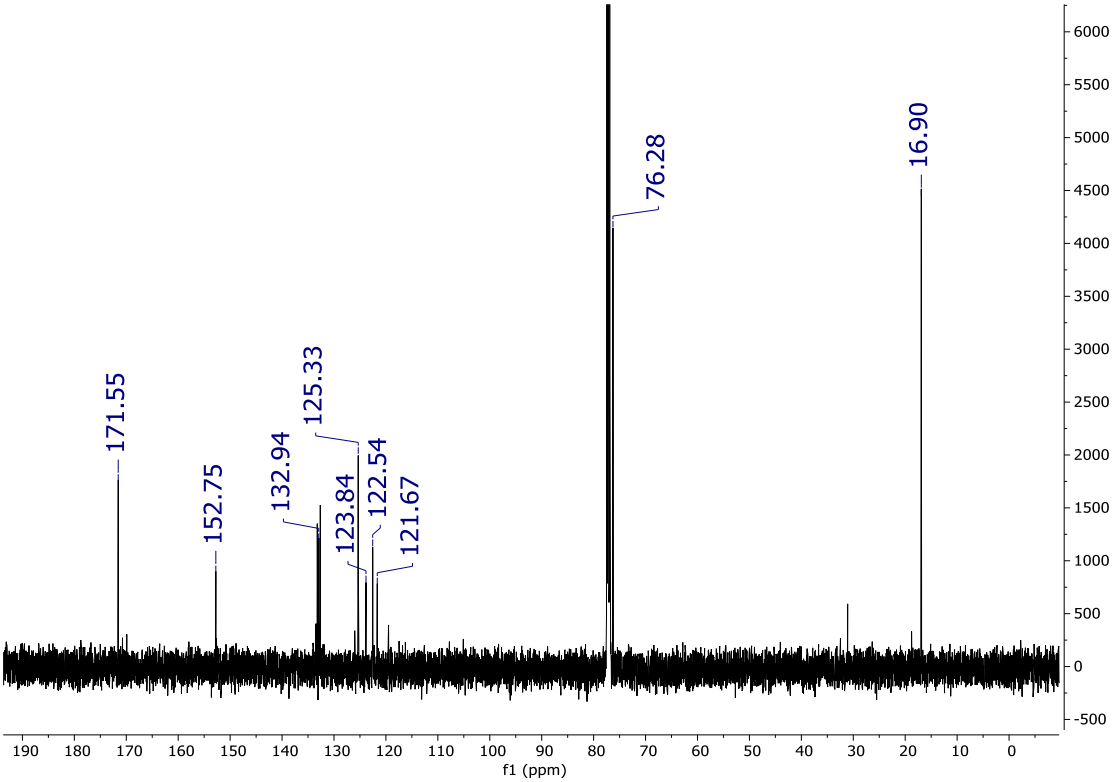

Fig. S51 $^{13}C\{H\}$ NMR spectrum ($CDCl_3$) of (S)-2-((3,5-bis(trifluoromethyl)phenyl)imino)-5-methyl-1,3−oxathiolan-4-one (residual chloroform peak at 77.16 ppm).

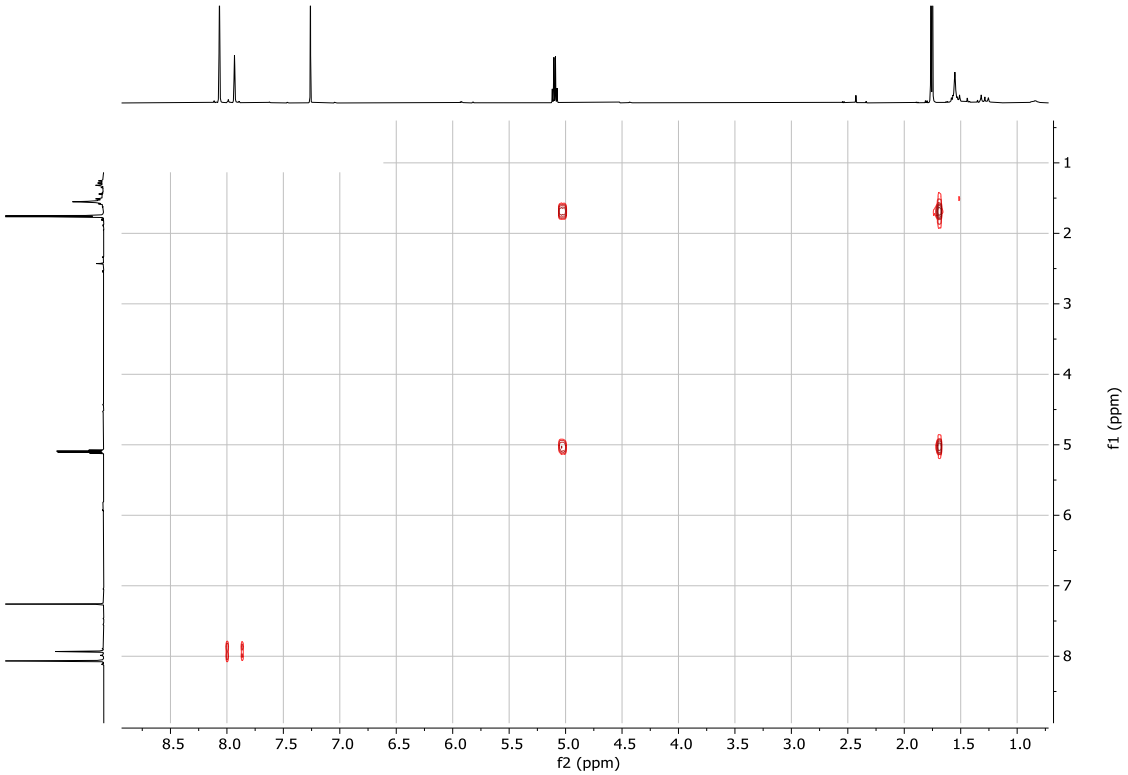

Fig. S52 ^{1}H COSY NMR spectrum ($CDCl_3$) of (S)-2-((3,5-bis(trifluoromethyl)phenyl)imino)-5-methyl-1,3−oxathiolan-4-one.

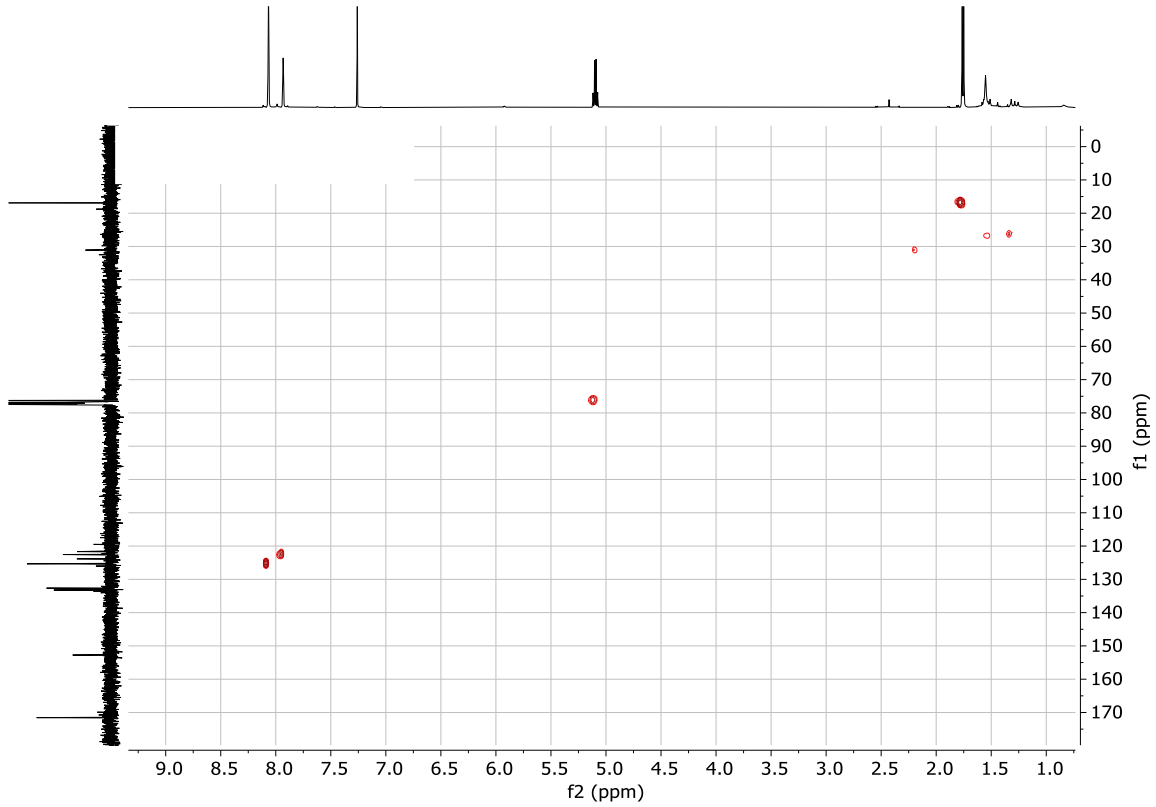

Fig. S53 ^{1}H-$^{13}C\{^{1}H\}$ HSQC NMR spectrum ($CDCl_3$) of (S)-2-((3,5-bis(trifluoromethyl)phenyl)imino)-5-methyl-1,3−oxathiolan-4-one.

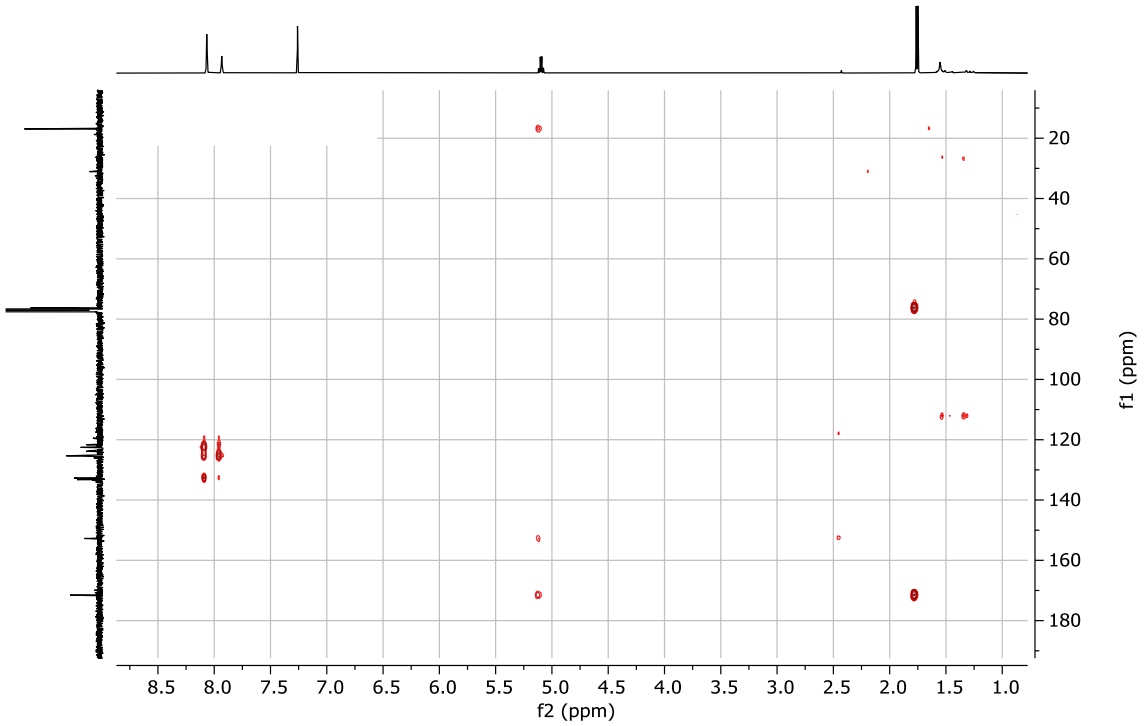

Fig. S54 ^{1}H-$^{13}C\{^{1}H\}$ HMBC NMR spectrum ($CDCl_3$) of (S)-2-((3,5-bis(trifluoromethyl)phenyl)imino)-5-methyl-1,3−oxathiolan-4-one.

9.2 Proposed mechanism for formation of oxathiolane product

Scheme S1. Proposed mechanism for the formation of oxathiolane product.

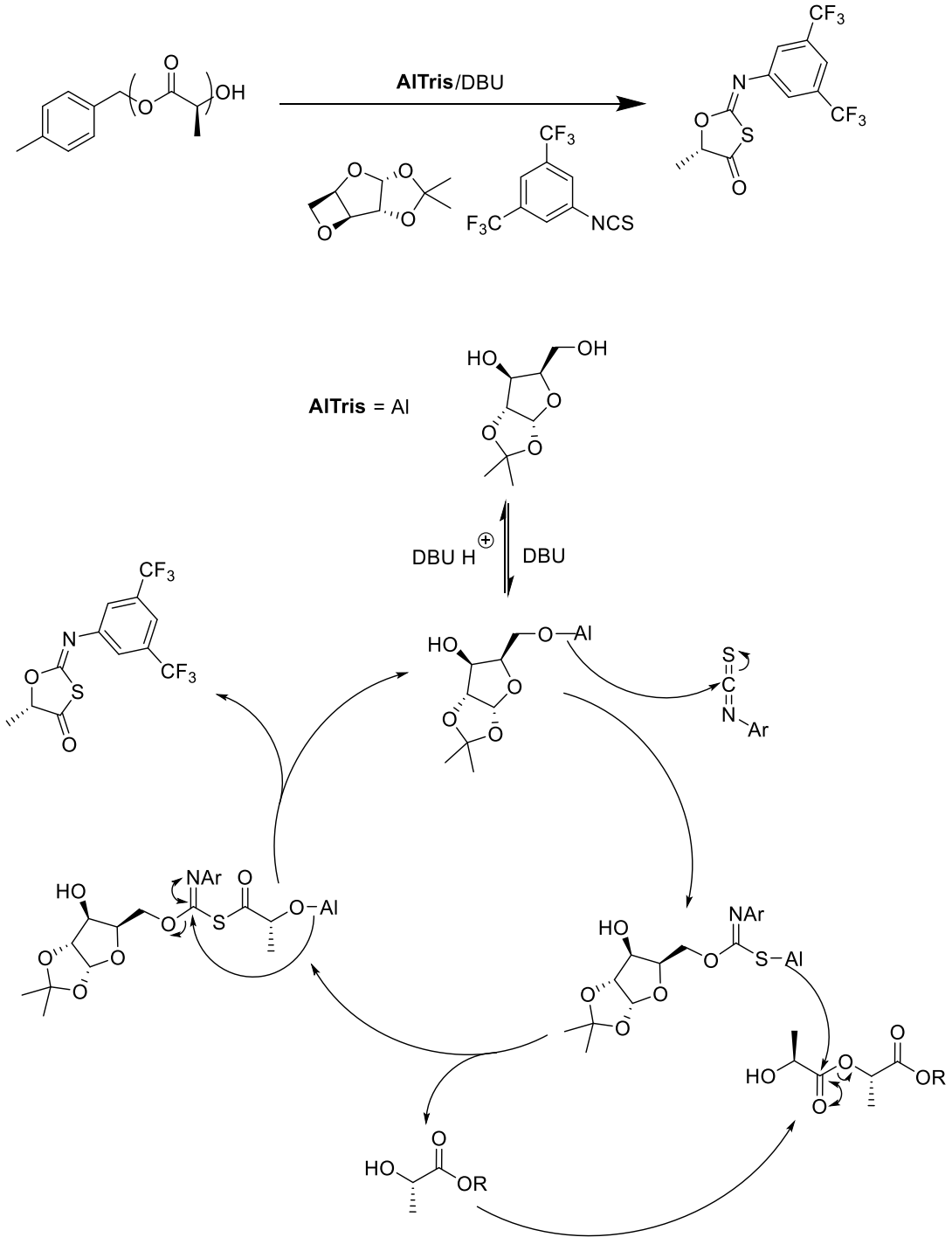

10 Metal Coordination

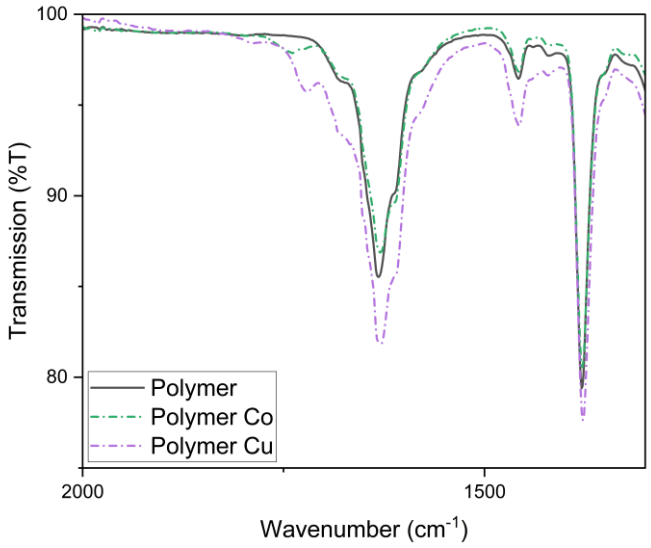

Fig. S55 FTIR spectra of poly(**D-Ox**-*alt*-**ITC1**) and isolated and dried poly(**D-Ox**-*alt*-**ITC1**) after stirring in solutions of Co and Cu.

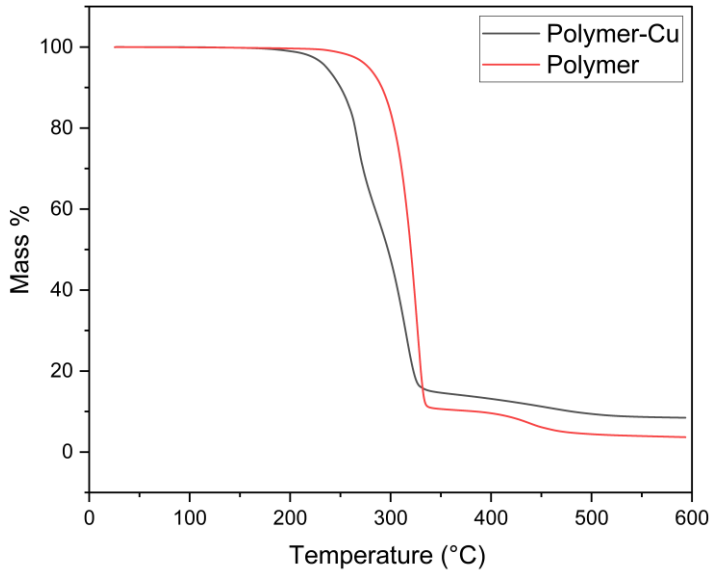

Fig. S56 TGA trace polymer-Cu and poly(**D-Ox**-*alt*-**ITC1**).

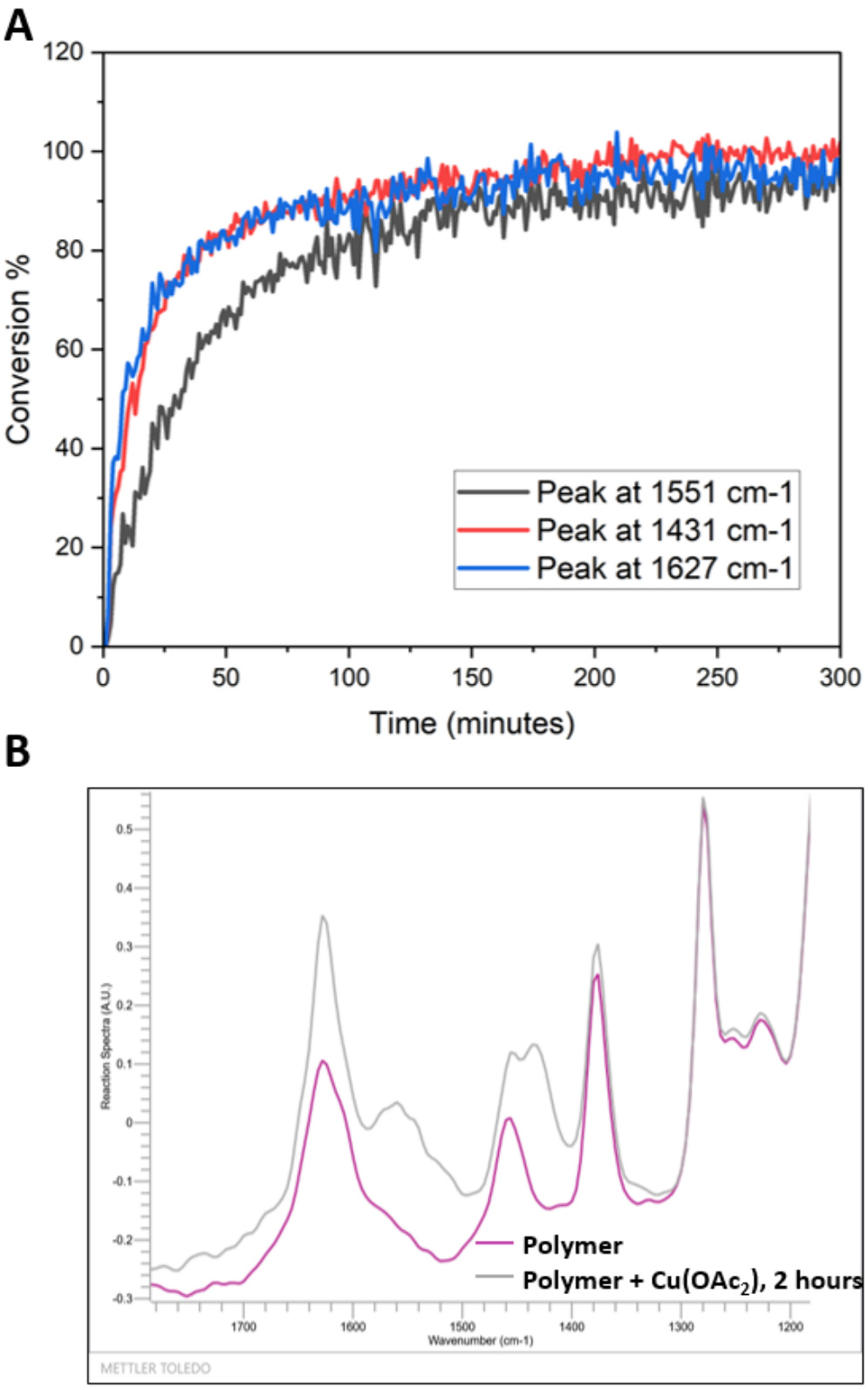

Fig. S57 Reaction carried out at [poly(D-**Ox**-*alt*-**ITC**)] = 1 mol L^{-1}, in THF at 50 °C with a ratio of poly(D-**Ox**-*alt*-**ITC**): $Cu(OAc_2)$ of 1:1. **(A)** Normalised conversion vs. time plot for the three poly(D-**Ox**-*alt*-**ITC**) wavenumbers : 1551 (–), 1431 (–) and 1627 (–) cm^{-1}. **(B)** FTIR spectra taken from Mettler Toledo software, at 0 and 2 hours.

11 References

1. T. M. McGuire, E. F. Clark and A. Buchard, *Macromolecules*, 2021, **54**, 5094-5105.
2. T. M. McGuire, J. Bowles, E. Deane, E. H. E. Farrar, M. N. Grayson and A. Buchard, *Angew. Chem. Int. Ed.*, 2021, **60**, 4524-4528.
3. C. J. Whiteoak, E. Martin, M. M. Belmonte, J. Benet-Buchholz and A. W. Kleij, *Adv. Synth.Catal.*, 2012, **354**, 469-476.
4. C. J. Whiteoak, N. Kielland, V. Laserna, F. Castro-Gómez, E. Martin, E. C. Escudero-Adán, C. Bo and A. W. Kleij, *Chem. Eur. J.*, 2014, **20**, 2264-2275.
5. H. S. Takuzo Aida, Masakatsu Kuroki and Shohei Inoue, *J. Phys. Org. Chem.*, 1995, **8**, 248-257.
6. CrysAlisPro 1.171.42.49 (Rigaku Oxford Diffraction, 2022), G. M. Sheldrick, *Acta Cryst.*, 2008, **64**, 112-122.